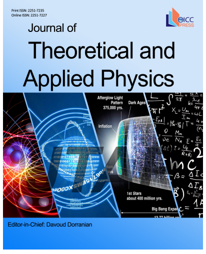

Volume 19, Issue 1, 192515 (1-29)

Journal of Theoretical and Applied Physics (JTAP)

https://doi.org/10.57647/j.jtap.2025.1901.15

Algebraic approaches for deriving soliton solutions and analyzing the stability of coupled Konno-Oono system arising in magnetic field

Umair Asghar[1], Muhammad Imran Asjad[1], Yahya Alsayaad[2,*], Yasser Salah Hamed[3]

[1] *Department of Mathematics, University of Management and Technology, Lahore, Pakistan.*
[2] *Department of Physics, Hodeidah University, Al-Hudaydah, Yemen.*
[3] *Department of Mathematics and Statistics, College of Science, Taif University, Taif, Saudi Arabia.*

*Corresponding authors: yahyaalsayyad2022@hoduniv.net.ye

Original Research

Received:
26 November 2024
Revised:
20 January 2024
Accepted:
26 January 2024
Published online:
10 February 2025

Abstract:

This article investigates the solutions of the new coupled Konno-Oono system arising in magnetic fields. In this respect, to explore analytical and physical behavior, by applying the two different techniques. The new extended direct algebraic technique and Nucci's direct reduction is used to obtain the different solutions of, new coupled Konno-Oono equation and these soliton type solutions as a singular, mixed singular, periodic, mixed trigonometric, complex combo, trigonometric, mixed hyperbolic, plane, and combined bright-dark soliton. To illustrate the propagation of certain solutions, the graphs associated to these solutions are displayed by selecting suitable parametric values in 3D, 2D as well as contour with the use of the symbolic software `Mathematica`. The visual representation of these findings proves invaluable in grasping the practical significance of the model equation under investigation. The acquired results represent a novel and broader perspective, showcasing the efficacy of the proposed method in analytically addressing nonlinear challenges in mathematical physics and engineering. They offer valuable insights into comprehending magnetic fields, ultimately contributing to the advancement of knowledge in this field. The modulation instability of the model is also discussed. Modulation instability is a versatile and powerful phenomenon of practical applications in scientific research. The computed solutions demonstrate that the methods employed are influential, efficient, and skillful, establishing them as a top choice for addressing non-linear equations in the context of magnetic fields.

Keywords: New extended direct algebraic approach; Nucci's direct reduction technique; New coupled Konno-Oono equation; Modulation instability

1. Introduction

Since the creation of the universe, there have been several extraordinary occurrences in a number of fields of life such as (plasma physics, optics, environmental science, chemistry, hydrodynamics, mathematical physics, and fluid mechanics and so forth). However, by cause of people are unaware of the source of these appearance and could not even capability they work and how to utilize these. Humankind could be creeping beyond technological advancement. Whenever partial differential equations were created (PDEs), that can be described numerous of those occurrences. However, even with all of these, the difficulty still exists since we are not able to understand the physical significance of these phenomena. Kruskal and Zabusky initially proposed the mean of soliton in 1965 and demonstrated how much each natural occurrence could be possible in several fields, enabling us to gain a lot of knowledge about the physical significance of this phenomenon [1–4]. The non-linear evolution equations (NLEEs) have recently turn the especially popular the theme of study in a wide range of fields for example, Atomic science, fluid mechanics, plasma physics, solid state, biology, cosmology, physics, ecology and so forth.

To properly understand non-linear phenomena, that is meaningful to obtain their exact solution and in addition to possible appliances in daily life. Soliton is a steady non-linear localized wave that retains their format as travelling through continuous velocities and depending on models, might be characterized as dark, solitary, or bright. In the non-linear sciences which play an important role in many physical phenomena [5]. On the other hand, earthquakes cause some stunning natural phenomena to happen especially, the seismic sea waves. The indicated wavelength and waves' peak scale is extremely significant. Furthermore, these waves produce incredible capacity should be transfigure within a suitable power source that can be indispensable years happening next. consequently, picking along with the consideration similar real troubles is essential into a mathematical physics [6]. Many fields of applied research, along with quantum mechanics, plasma physics, economics, shallow water wave propagation, electromagnetic theory, meteorology, chemical kinetics solid state physics, optics, fluid dynamics, ecology, and so on, depend heavily on NLPDEs see [7–12]. Because the nonlinear wave equations are so complicated, more and more people are now becoming interested in investigating the travelling wave solutions. Therefore, with the quick growth of symbolic computational systems.

Mathematicians and physicists have effectively presented and constructed a variety of new methodologies. For instance, auxiliary equation methodology [13], Painlevé analysis method [14, 15], Riccati-Bernoulli sub-ODE technique [16], modified Kudryashov methodology [17], exponential function methodology [18], Darboux transformations [19–22], sine-Gordon expansion methodology [23], algebra technique [24], tanh-sech technique [25], sub-equation technique [26], sine–cosine technique [27], Jacobi elliptic function methodology [28], homotopy perturbation [29], variational iteration technique [30], first integral methodology [31], trial solution methodology [32], $\frac{G'}{G}$-expansion methodology [33], Studies on solitons have recently spotted the interest of different analysts from all around the world [34–39]. Independently introduced was the recommended theme, which is a major element in the magnetic field profile by K. Konno and H. Oono [40–42]. As applications for present-field strings connecting with exterior magnetic field systems.

A current-fed string defined by a new coupled Konno-Oono equation which interacts along with the exterior magnetic field in three dimensions of Euclidean space. Developed a more generalized form of the coupled integrable dispersion less system in 1990, which is described as. The coupled integrable dispersion less system is used to present the nonlinear CKO equation in [43]. These equations are derived from the principles of conservation laws and nonlinear wave theory, encapsulating the complex interplay between nonlinearity and dispersion. This makes the system an excellent candidate for testing the effectiveness of advanced analytical techniques.

$$
\begin{aligned}
&J_{xt} - 2\chi_1 J W_{xx} - 2\chi_2 J K_x + \chi_3 (WK)_x = 0,\\
&W_{xt} - 2\chi_1 W W_x - 2\chi_2 (2JJ_x + W_x K) - 2\chi_3 (J)_x W = 0,\\
&K_{xt} - 2\chi_2 K K_x - 2\chi_1 (2JJ_x + K_x W) - 2\chi_3 (J)_x K = 0.
\end{aligned} \tag{1}
$$

Where χ_1, χ_2 and χ_3 are arbitrary constants. This system describes the interaction of a magnetic field as well as a current-fed string in three dimensions. When such particular values are chosen, that's network transforms into a new Konno-Oono equation coupled network of integrable dispersion free equations [5],

$$
\begin{aligned}
&\Phi_{xt} - 2\Psi\Phi = 0,\\
&\Psi_t + 2\Phi\Phi_x = 0.
\end{aligned} \tag{2}
$$

With some mathematical relationships, several researchers have investigated and examined this system in connection to various new and different properties. The sine-Gordon expansion approach [44], the extended exp function [45], the external trial equation [46], and the tanh-function and extended tanh-function techniques [47], all could be used to study this system in recent years. The coupled Konno-Oono system arising in magnetic fields, we know that Magnetic fields are intimately related to electromagnetic waves. Electromagnetic waves are a form of energy transfer in the form of oscillating electric and magnetic fields that propagate through space. These waves are generated when an electric charge accelerates, creating a changing electric field, which, in turn, generates a changing magnetic field. These changing electric and magnetic fields then feed off each other as they move through space, creating a self-sustaining wave [48]. These waves can occur in various physical systems, including water, optical fibers, and plasmas. In the context of plasmas, where magnetic fields play a significant role, soliton-like structures can emerge. These are often referred to as magnetic solitons or magnetic solitary waves. The solitons in birefringent optical fibers with Hamiltonian perturbations and Kerr law nonlinearity [49]. The enhanced Kudryashov's and general projective Riccati equations techniques for obtaining exact solutions to the fifth-order nonlinear water wave (FONLWWE) equation [50]. A new simple integration technique to extract optical solitons for the cubic quartic Bragg-gratings having anti-cubic nonlinear form [51]. Dispersive optical solitons are naturally present in optical fibers whenever there is a dominance of third order and fourth order dispersion in addition to nonlinear dispersion. One particular type of optical fiber that appears with parabolic law nonlinearity and is also visible in sulfonate crystals [52]. The system models the propagation of magneto-hydrodynamic waves and the interaction of magnetic fields with plasma flows. It captures the dynamics of wave interactions where magnetic forces and nonlinear effects are prominent, making it a vital framework for understanding such scenarios in applied physics and engineering.

Recently, Rehman et al. [5], examine the new coupled Konno–Oono (CKO) equation and employed the Sardar Subequation Approach to obtain soliton type results in the development of dark, bright, periodic singular, mixed solutions, and singular.

Rehman can not explain the modulation instability and their failure to provide an explanation for the solutions presented in this article have left a significant knowledge gap. Within this work, numerous solutions have been concealed, and it is imperative to address this deficiency. By doing so, we aim to bridge the void in our understanding, ensuring that the undisclosed solutions are comprehensively elucidated, and the potential insights they offer are fully realized. This effort to fill the gap will enhance the depth and completeness of the research, making it more valuable to the scientific community and advancing our understanding of the subject matter. Based on our current understanding, we have successfully obtained an array of diverse solutions associating with magnetic field, including singular solutions, complex solitary shock solutions, mixed singular solutions, shock singular solitons, mixed trigonometric solutions, shock solutions, complex combination solutions, periodic trigonometric solutions, mixed periodic solutions, hyperbolic solutions, as well as combined bright-dark and periodic solutions. In this research, we have introduced and refined these novel solutions, contributing to the existing body of knowledge and expanding the available solutions for the problem at hand. Our work adds value by unveiling these new and enhanced solutions, which offer valuable insights into the subject matter. While Rehman did not address the topic of modulation instability, our work has rectified this gap by providing a comprehensive description and a concise explanation of modulation instability. This addition serves to enhance the comprehensiveness of our research, filling the gap that existed in the understanding of this phenomenon.

The primary objective of this article is to provide exact solutions for the recently formulated coupled Konno-Oono equation within the context of a magnetic field. In pursuit of this goal, we have harnessed the power of generalized expansion schemes, which have allowed us to explore new frontiers and unveil fresh findings in the field. Our study hinges on two pivotal methodologies, each with its distinct strengths and contributions. The first method is an innovative extension of the direct algebraic approach, which has yielded an impressive total of thirty-seven diverse solutions. These solutions are not only numerous but also distinct from one another, rendering them invaluable for advancing research and fostering a more comprehensive understanding of the problem at hand. They open up exciting avenues for further exploration and application. Furthermore, we have employed Nucci's direct reduction technique as our second methodology. Through this approach, we have achieved the acquisition of exact solutions, which stand as significant contributions to the broader body of knowledge in this area. These exact solutions are crucial in refining our understanding and facilitating practical applications within the domain of the Konno-Oono equation in a magnetic field. Following the implementation of this scheme, we have successfully obtained combined bright-dark soliton and periodic soliton solutions. These findings hold substantial practical significance at the industrial level, offering valuable tools and insights for various applications. In addition to presenting our findings, we have included graphical representations to further illustrate the significance of our results. These novel outcomes are highly relevant and beneficial in the realm of applied sciences, opening up new avenues for practical applications. Scientists exploring this specific system will find that the methods we discuss are not only robust but also highly effective in deriving solitary wave solutions, enhancing their toolkit for tackling complex problems. The stability of our model has been addressed through an examination of modulation instability. Modulation instability is of paramount importance as it provides critical insights into the stability and behavior of our model. It helps us understand how small perturbations or variations in our system evolve over time and impact its overall stability and performance. This understanding is invaluable for assessing the reliability and robustness of our model, as well as for making informed decisions about its real-world applications and implications. The coupled Konno-Oono system arising in a magnetic field offers substantial industrial benefits. This system's practical utility spans across various industrial applications, where its precise solutions can enhance processes, optimize designs, and contribute to the advancement of technology. By harnessing the insights derived from this system, industries can improve efficiency, develop innovative products, and achieve a competitive edge. The solutions obtained from this system serve as valuable tools for engineers and researchers, enabling them to tackle complex problems and pave the way for new, industrially relevant developments in science and technology.

In section 2, the analytical methods are described and important information to utilize methodologies are explained. In the next portion 3, 4, the application of the given model will be derived by new extended direct algebraic methodology and Nucci's direct reduction scheme together with also shown the graphical representation. In section 5, the graphical explanation is given. Furthermore, modulation instability is explained in section 6. In the end the conclusions 7 will be demonstrated.

2. Description of the analytical methods

The suggested approaches are successfully pertinent to complex non-linear dominant structures.

Let a non-linear partial differential equation [53]:

$$\mathscr{F}(\phi, \phi_x, \phi_t, \phi_{xt}, \phi_{xx}, \ldots) = 0, \tag{3}$$

where, $\mathscr{F}$ is the polynomial in $\phi = \phi(x,t)$ is an unspecified function and it's partial derivatives.

That converts through the ordinary differential equation [54]:

$$\mathscr{J}(\mathbb{H}, \mathbb{H}', \mathbb{H}'', \ldots) = 0. \tag{4}$$

Apply the transformation is given:

$$\phi(x,t) = \mathbb{H}(\psi), \tag{5}$$

where, $\psi = a_1 x + a_2 t$. a_1 and a_2 are constant and it can be adjusted according to the model.

3. New extended direct algebraic method

Let Eq. (4) has solutions as [55–58]:

$$\mathbb{H}(\psi) = \sum_{j=0}^{m} \left[d_j (\mathbb{L}(\psi))^j \right], \; d_m \neq 0, \tag{6}$$

where d_j $0 \le j \le m$ are constant coefficients to be evaluated later; m is a positive integer, which is found by the balancing principle in Eq. (5) and $\mathbb{L}'(\psi)$ holds the ODE in the form,

$$\mathbb{L}'(\psi) = \log[\varepsilon] \left(\alpha + \beta \mathbb{L}(\psi) + \gamma \mathbb{L}^2(\psi) \right), \quad 0 < \varepsilon \neq 1, \tag{7}$$

where, α, β and γ are real constants. The general roots concerning to parameters α, β and γ of Eq. (7) are: (Class 1): When $\gamma \neq 0$, and $\beta^2 - 4\alpha\gamma < 0$,

$$\mathbb{L}_1(\psi) = -\frac{\beta}{2\gamma} + \frac{\sqrt{-(\beta^2 - 4\alpha\gamma)}}{2\gamma} \tan_\varepsilon \left(\frac{\sqrt{-(\beta^2 - 4\alpha\gamma)}}{2} \psi \right), \tag{8}$$

$$\mathbb{L}_2(\psi) = -\frac{\beta}{2\gamma} - \frac{\sqrt{-(\beta^2 - 4\alpha\gamma)}}{2\gamma} \cot_\varepsilon \left(\frac{\sqrt{-(\beta^2 - 4\alpha\gamma)}}{2} \psi \right), \tag{9}$$

$$\mathbb{L}_3(\psi) = -\frac{\beta}{2\gamma} + \frac{\sqrt{-(\beta^2 - 4\alpha\gamma)}}{2\gamma} \left(\tan_\varepsilon \left(\sqrt{-(\beta^2 - 4\alpha\gamma)} \psi \right) \pm \sqrt{mn} \sec_\varepsilon \left(\sqrt{-(\beta^2 - 4\alpha\gamma)} \psi \right) \right), \tag{10}$$

$$\mathbb{L}_4(\psi) = -\frac{\beta}{2\gamma} + \frac{\sqrt{-(\beta^2 - 4\alpha\gamma)}}{2\gamma} \left(\cot_\varepsilon \left(\sqrt{-(\beta^2 - 4\alpha\gamma)} \psi \right) \pm \sqrt{mn} \csc_\varepsilon \left(\sqrt{-(\beta^2 - 4\alpha\gamma)} \psi \right) \right), \tag{11}$$

$$\mathbb{L}_5(\psi) = -\frac{\beta}{2\gamma} + \frac{\sqrt{-(\beta^2 - 4\alpha\gamma)}}{4\gamma} \left(\tan_\varepsilon \left(\frac{\sqrt{-(\beta^2 - 4\alpha\gamma)}}{4} \psi \right) - \cot_\varepsilon \left(\frac{\sqrt{-(\beta^2 - 4\alpha\gamma)}}{4} \psi \right) \right). \tag{12}$$

(Class 2): When $\gamma \neq 0$, and $\beta^2 - 4\alpha\gamma > 0$,

$$\mathbb{L}_6(\psi) = -\frac{\beta}{2\gamma} - \frac{\sqrt{\beta^2 - 4\alpha\gamma}}{2\gamma} \tanh_\varepsilon \left(\frac{\sqrt{\beta^2 - 4\alpha\gamma}}{2} \psi \right), \tag{13}$$

$$\mathbb{L}_7(\psi) = -\frac{\beta}{2\gamma} - \frac{\sqrt{\beta^2 - 4\alpha\gamma}}{2\gamma} \coth_\varepsilon \left(\frac{\sqrt{\beta^2 - 4\alpha\gamma}}{2} \psi \right), \tag{14}$$

$$\mathbb{L}_8(\psi) = -\frac{\beta}{2\gamma} + \frac{\sqrt{\beta^2 - 4\alpha\gamma}}{2\gamma} \left(-\tanh_\varepsilon \left(\sqrt{\beta^2 - 4\alpha\gamma} \psi \right) \pm i \sqrt{mn} sech_\varepsilon \left(\sqrt{\beta^2 - 4\alpha\gamma} \psi \right) \right), \tag{15}$$

$$\mathbb{L}_9(\psi) = -\frac{\beta}{2\gamma} + \frac{\sqrt{\beta^2 - 4\alpha\gamma}}{2\gamma} \left(-\coth_\varepsilon \left(\sqrt{\beta^2 - 4\alpha\gamma} \psi \right) \pm \sqrt{mn} csch_\varepsilon \left(\sqrt{\beta^2 - 4\alpha\gamma} \psi \right) \right), \tag{16}$$

$$\mathbb{L}_{10}(\psi) = -\frac{\beta}{2\gamma} - \frac{\sqrt{\beta^2 - 4\alpha\gamma}}{4\gamma} \left(tanh_\varepsilon \left(\frac{\sqrt{\beta^2 - 4\alpha\gamma}}{4} \psi \right) + coth_\varepsilon \left(\frac{\sqrt{\beta^2 - 4\alpha\gamma}}{4} \psi \right) \right). \tag{17}$$

(Class 3): When $\beta = 0$ and $\alpha\gamma > 0$,

$$\mathbb{L}_{11}(\psi) = \sqrt{\frac{\alpha}{\gamma}}\, tan_{\varepsilon}\left(\sqrt{\alpha\gamma}\psi\right), \tag{18}$$

$$\mathbb{L}_{12}(\psi) = -\sqrt{\frac{\alpha}{\gamma}}\, cot_{\varepsilon}\left(\sqrt{\alpha\gamma}\psi\right), \tag{19}$$

$$\mathbb{L}_{13}(\psi) = \sqrt{\frac{\alpha}{\gamma}}\left(\tan_{\varepsilon}\left(2\sqrt{\alpha\gamma}\psi\right) \pm \sqrt{mn}\, sec_{\varepsilon}\left(2\sqrt{\alpha\gamma}\psi\right)\right), \tag{20}$$

$$\mathbb{L}_{14}(\psi) = \sqrt{\frac{\alpha}{\gamma}}\left(-\, cot_{\varepsilon}\left(2\sqrt{\alpha\gamma}\psi\right) \pm \sqrt{mn}\csc_{\varepsilon}\left(2\sqrt{\alpha\gamma}\psi\right)\right), \tag{21}$$

$$\mathbb{L}_{15}(\psi) = \frac{1}{2}\sqrt{\frac{\alpha}{\gamma}}\left(\tan_{\varepsilon}\left(\frac{\sqrt{\alpha\gamma}}{2}\psi\right) - \cot_{\varepsilon}\left(\frac{\sqrt{\alpha\gamma}}{2}\psi\right)\right). \tag{22}$$

(Class 4): When $\beta = 0$ and $\alpha\gamma < 0$,

$$\mathbb{L}_{16}(\psi) = -\sqrt{-\frac{\alpha}{\gamma}}\tanh_{\varepsilon}\left(\sqrt{-\alpha\gamma}\psi\right), \tag{23}$$

$$\mathbb{L}_{17}(\psi) = -\sqrt{-\frac{\alpha}{\gamma}}\coth_{\varepsilon}\left(\sqrt{-\alpha\gamma}\psi\right), \tag{24}$$

$$\mathbb{L}_{18}(\psi) = \sqrt{-\frac{\alpha}{\gamma}}\left(-\tanh_{\varepsilon}\left(2\sqrt{-\alpha\gamma}\psi\right) \pm i\sqrt{mn} sech_{\varepsilon}\left(2\sqrt{-\alpha\gamma}\psi\right)\right), \tag{25}$$

$$\mathbb{L}_{19}(\psi) = \sqrt{-\frac{\alpha}{\gamma}}\left(-\coth_{\varepsilon}\left(2\sqrt{-\alpha\gamma}\psi\right) \pm \sqrt{mn} csch_{\varepsilon}\left(2\sqrt{-\alpha\gamma}\psi\right)\right), \tag{26}$$

$$\mathbb{L}_{20}(\psi) = -\frac{1}{2}\sqrt{-\frac{\alpha}{\gamma}}\left(\tanh_{\varepsilon}\left(\frac{\sqrt{-\alpha\gamma}}{2}\psi\right) + \, coth_{\varepsilon}\left(\frac{\sqrt{-\alpha\gamma}}{2}\psi\right)\right). \tag{27}$$

(Class 5): When $\beta = 0$ and $\alpha = \gamma$,

$$\mathbb{L}_{21}(\psi) = \tan_{\varepsilon}(\alpha\psi), \tag{28}$$

$$\mathbb{L}_{22}(\psi) = -\cot_{\varepsilon}(\alpha\psi), \tag{29}$$

$$\mathbb{L}_{23}(\psi) = \tan_{\varepsilon}(2\alpha\psi) \pm \sqrt{mn}\sec_{\varepsilon}(2\alpha\psi), \tag{30}$$

$$\mathbb{L}_{24}(\psi) = -\cot_{\varepsilon}(2\alpha\psi) \pm \sqrt{mn}\csc_{\varepsilon}(2\alpha\psi), \tag{31}$$

$$\mathbb{L}_{25}(\psi) = \frac{1}{2}\left(\tan_{\varepsilon}\left(\frac{\alpha}{2}\psi\right) - \cot_{\varepsilon}\left(\frac{\alpha}{2}\psi\right)\right). \tag{32}$$

(Class 6): When $\gamma = -\alpha$ and $\beta = 0$,

$$\mathbb{L}_{26}(\psi) = -\tanh_{\varepsilon}(\alpha\psi), \tag{33}$$

$$\mathbb{L}_{27}(\psi) = -\coth_{\varepsilon}(\alpha\psi), \tag{34}$$

$$\mathbb{L}_{28}(\psi) = -\tanh_{\varepsilon}(2\alpha\psi) \pm i\sqrt{mn} sech_{\varepsilon}(2\alpha\psi), \tag{35}$$

$$\mathbb{L}_{29}(\psi) = -\cot_\varepsilon(2\alpha\psi) \pm \sqrt{mn}\, csch_\varepsilon(2\alpha\psi), \tag{36}$$

$$\mathbb{L}_{30}(\psi) = -\frac{1}{2}\left(\tanh_\varepsilon\left(\frac{\alpha}{2}\psi\right) + \coth_\varepsilon\left(\frac{\alpha}{2}\psi\right)\right). \tag{37}$$

(Class 7): When $\beta^2 = 4\alpha\gamma$,

$$\mathbb{L}_{31}(\psi) = \frac{-2\alpha(\beta\psi\log[\varepsilon] + 2)}{\beta^2\psi\log[\varepsilon]}. \tag{38}$$

(Class 8): When $\alpha = pq, (q \neq 0), \beta = p$, and $\gamma = 0$,

$$\mathbb{L}_{32}(\psi) = \varepsilon^{p\psi} - q. \tag{39}$$

(class 9): When $\beta = \gamma = 0$,

$$\mathbb{L}_{33}(\psi) = \alpha\psi\log[\varepsilon]. \tag{40}$$

(class 10): When $\beta = \alpha = 0$,

$$\mathbb{L}_{34}(\psi) = \frac{-1}{\gamma\psi\log[\varepsilon]}. \tag{41}$$

(Class 11): When $\alpha = 0$ and $\beta \neq 0$,

$$\mathbb{L}_{35}(\psi) = -\frac{m\beta}{\gamma(\cosh_\varepsilon(\beta\psi) - \sinh_\varepsilon(\beta\psi) + m)}, \tag{42}$$

$$\mathbb{L}_{36}(\psi) = -\frac{\beta(\sinh_\varepsilon(\beta\psi) + \cosh_\varepsilon(\beta\psi))}{\gamma(\sinh_\varepsilon(\beta\psi) + \cosh_\varepsilon(\beta\psi) + n)}. \tag{43}$$

(Class 12): When $\gamma = pq$, $(q \neq 0)$, $\beta = p$, and $\alpha = 0$,

$$\mathbb{L}_{37}(\psi) = -\frac{m\varepsilon^{p\psi}}{m - qn\varepsilon^{p\psi}}. \tag{44}$$

Here the generalized hyperbolic and trigonometric functions are defined as [59],

$$\sinh_\varepsilon(\psi) = \frac{m\varepsilon^{\psi} - n\chi^{-\psi}}{2},\ \cosh_\varepsilon(\psi) = \frac{m\varepsilon^{\psi} + n\varepsilon^{-\psi}}{2},$$

$$\tanh_\varepsilon(\psi) = \frac{m\varepsilon^{\psi} - n\varepsilon^{-\psi}}{m\varepsilon^{\psi} + n\varepsilon^{-\psi}},\ \coth_\varepsilon(\psi) = \frac{m\varepsilon^{\psi} + n\varepsilon^{-\psi}}{m\varepsilon^{\psi} - n\varepsilon^{-\psi}},$$

$$sech_\varepsilon(\psi) = \frac{2}{m\varepsilon^{\psi} + n\varepsilon^{-\psi}},\ csch_\varepsilon(\psi) = \frac{2}{m\varepsilon^{\psi} - n\varepsilon^{-\psi}},$$

$$sin_\varepsilon(\psi) = \frac{m\varepsilon^{i\psi} - n\varepsilon^{-i\psi}}{2i},\ \ cos_\varepsilon(\psi) = \frac{m\varepsilon^{i\psi} + n\varepsilon^{-i\psi}}{2},$$

$$\tan_\varepsilon(\psi) = -i\frac{m\varepsilon^{i\psi} - n\varepsilon^{-i\psi}}{m\varepsilon^{i\psi} + n\varepsilon^{-i\psi}},\ \ \cot_\varepsilon(\psi) = i\frac{m\varepsilon^{i\psi} + n\varepsilon^{-i\psi}}{m\varepsilon^{i\psi} - n\varepsilon^{-i\psi}},$$

where $m, n > 0$ are arbitrary constant deformation parameters.

3.1 Nucci's reduction approach

This method of operation is distinct out of the earlier one. The present technique, look over the exact solutions of the derived single nonlinear ODE Eq. (4). The analogous effective model of derived ODE is derived. Eventually selecting a dependent parameter of structure, a single first order separable ODE if obtained. Solve this equation and return the choosing variables independent variable, one gets the ending out comes. Some first integrals are extracted, by utilize this method.

4. Construction of analytical solutions

4.1 Application of new extended direct algebraic method

In this section, we could pertain the new extended distinct algebraic mechanism. To extract solutions of the Eq. (2) we set up a traveling wave transformation:

$$\begin{aligned}\Phi(x,t)&=\mathbb{M}(\psi),\psi=v(x-\xi t),\\ \Psi(x,t)&=\mathbb{P}(\psi),\psi=v(x-\xi t),\end{aligned}\tag{45}$$

where, ξ and v are the velocity and wave number. By putting the Eq. (45) in to the Eq. (2) we obtain the following ODEs,

$$\xi v^2\mathbb{M}''+2\mathbb{P}\mathbb{M}=0,\tag{46}$$

$$\xi v\mathbb{P}'+2v\mathbb{M}\mathbb{M}'=0.\tag{47}$$

Now, integrating the Eq. (47) with respect to ψ, we acquire,

$$\mathbb{P}=\frac{1}{\xi}\left(\mathbb{M}^2+\delta\right),\tag{48}$$

where, δ is an integration constant. By putting Eq. (48) into an Eq. (46), we get,

$$\xi^2v^2\mathbb{M}''+2\mathbb{M}^3+2\delta\mathbb{M}=0.\tag{49}$$

Now, by balancing constant $\mathbb{M}^3$ and $\mathbb{M}''$ in above Eq. (49) we get $j=1$. So it offers a series from Eq. (6) as:

$$\mathbb{M}(\psi)=d_0+d_1(\mathbb{L}(\psi)).\tag{50}$$

Recognize the coefficient of the different powers,

$$\begin{aligned}&\mathbb{L}(\psi)^0:\xi^2v^2d_1\beta\,(\ln(\varepsilon))^2\alpha+2d_0{}^3+2\,\delta\,d_0=0.\\ &\mathbb{L}(\psi)^1:\xi^2v^2d_1\beta^2(\ln(\varepsilon))^2+2\xi^2v^2d_1\gamma(\ln(\varepsilon))^2\alpha+6d_0{}^2d_1+2\,\delta\,d_1=0.\\ &\mathbb{L}(\psi)^2:3\,\xi^2v^2d_1\beta\,(\ln(\varepsilon))^2\gamma+6d_0d_1{}^2=0.\\ &\mathbb{L}(\psi)^3:2\,\xi^2v^2d_1\gamma^2(\ln(\varepsilon))^2+2d_1{}^3=0.\end{aligned}\tag{51}$$

The solution of upper model Eq. (51) is acquired along the support of `Mathematica`,

$$\left[\xi=\pm\frac{2\sqrt{\delta}}{\sqrt{v^2(\Lambda)log[\varepsilon]^2}},d_0=\pm\iota\Delta\beta,d_1=\pm2\iota\Delta\gamma\right],\tag{52}$$

where,

$$\Delta=\pm\frac{\sqrt{\delta}}{\sqrt{\Lambda}},\Lambda=\beta^2-4\alpha\gamma,\iota=\sqrt{-1}.\tag{53}$$

The general solution of Eq. (2) is obtained,

$$\begin{aligned}\Phi(x,t)&=\iota\Delta\left(\beta+2\gamma(\mathbb{L}_i(\psi))\right),\\ \Psi(x,t)&=\frac{1}{\xi}\left(\delta-\Delta^2\left(\beta+2\gamma(\mathbb{L}_i(\psi))\right)^2\right).\end{aligned}\tag{54}$$

Since, we have to extract various unlike solutions by taking $\mathbb{L}_i$ from the Eq. (8) to Eq. (44) respecting. We will obtain the unlike solutions of different forms as follows.
(Class 1): As $\beta^2-4\alpha\gamma<0$, and $\gamma\neq0$, then mixed trigonometric solutions are acquired,

$$\Phi_1(x,t)=\pm\Delta\sqrt{\beta^2-4\alpha\gamma}\tan_{\varepsilon}\left(\frac{\sqrt{-(\beta^2-4\alpha\gamma)}}{2}v(x-\xi t)\right),\tag{55}$$

$$\Psi_1(x,t)=\frac{1}{\xi}\left(\delta+\Delta^2(\beta^2-4\alpha\gamma)\tan^2_{\varepsilon}\left(\frac{\sqrt{-(\beta^2-4\alpha\gamma)}}{2}v(x-\xi t)\right)\right),\tag{56}$$

$$\Phi_2(x,t) = \mp\Delta\sqrt{(\beta^2-4\alpha\gamma)}\cot_\varepsilon\left(\frac{\sqrt{-(\beta^2-4\alpha\gamma)}}{2}v(x-\xi t)\right), \tag{57}$$

$$\Psi_2(x,t) = \frac{1}{\xi}\left(\delta+\Delta^2(\beta^2-4\alpha\gamma)\cot^2_\varepsilon\left(\frac{\sqrt{-(\beta^2-4\alpha\gamma)}}{2}v(x-\xi t)\right)\right), \tag{58}$$

$$\Phi_3(x,t) = \pm\Delta\sqrt{(\beta^2-4\alpha\gamma)}\left(\tan_\varepsilon\left(\sqrt{-(\beta^2-4\alpha\gamma)}\psi\right)\pm\sqrt{mn}\sec_\varepsilon\left(\sqrt{-(\beta^2-4\alpha\gamma)}v(x-\xi t)\right)\right) \tag{59}$$

$$\Psi_3(x,t) = \frac{1}{\xi}\left(\delta+\Delta^2(\beta^2-4\alpha\gamma)\left(\tan_\varepsilon\left(\sqrt{-(\beta^2-4\alpha\gamma)}\psi\right)\pm\sqrt{mn}\sec_\varepsilon\left(\sqrt{-(\beta^2-4\alpha\gamma)}v(x-\xi t)\right)\right)^2\right), \tag{60}$$

$$\Phi_4(x,t) = \mp\Delta\sqrt{-(\beta^2-4\alpha\gamma)}\left(\cot_\varepsilon\left(\sqrt{-(\beta^2-4\alpha\gamma)}\psi\right)\pm\sqrt{mn}\csc_\varepsilon\left(\sqrt{-(\beta^2-4\alpha\gamma)}v(x-\xi t)\right)\right), \tag{61}$$

$$\Psi_4(x,t) = \frac{1}{\xi}\left(\delta\Delta^2(\beta^2-4\alpha\gamma)\left(\cot_\varepsilon\left(\sqrt{-(\beta^2-4\alpha\gamma)}\psi\right)\pm\sqrt{mn}\csc_\varepsilon\left(\sqrt{-(\beta^2-4\alpha\gamma)}v(x-\xi t)\right)\right)^2\right), \tag{62}$$

$$\Phi_5(x,t) = \pm\frac{\Delta\sqrt{(\beta^2-4\alpha\gamma)}}{2}\left(\tan_\varepsilon\left(\frac{\sqrt{-(\beta^2-4\alpha\gamma)}}{4}\psi\right)-\cot_\varepsilon\left(\frac{\sqrt{-(\beta^2-4\alpha\gamma)}}{4}v(x-\xi t)\right)\right), \tag{63}$$

$$\Psi_5(x,t) = \frac{1}{\xi}\left(\delta+\frac{\Delta^2(\beta^2-4\alpha\gamma)\left(\tan_\varepsilon\left(\frac{\sqrt{-(\beta^2-4\alpha\gamma)}}{4}\psi\right)-\sqrt{mn}\cot_\varepsilon\left(\frac{\sqrt{-(\beta^2-4\alpha\gamma)}}{4}v(x-\xi t)\right)\right)^2}{4}\right). \tag{64}$$

(Class 2): As $\beta^2-4\alpha\gamma>0$, and $\gamma\neq 0$, we obtained the solutions of various kinds as follows.
The shock solution is achieved,

$$\Phi_6(x,t) = \pm\imath\Delta\sqrt{\beta^2-4\alpha\gamma}\tanh_\varepsilon\left(\frac{\sqrt{\beta^2-4\alpha\gamma}}{2}v(x-\xi t)\right), \tag{65}$$

$$\Psi_6(x,t) = \frac{1}{\xi}\left(\delta-\Delta^2(\beta^2-4\alpha\gamma)\tanh^2_\varepsilon\left(\frac{\sqrt{\beta^2-4\alpha\gamma}}{2}v(x-\xi t)\right)\right). \tag{66}$$

The singular solution is derived as,

$$\Phi_7(x,t) = \pm\imath\Delta\sqrt{\beta^2-4\alpha\gamma}\coth_\varepsilon\left(\frac{\sqrt{\beta^2-4\alpha\gamma}}{2}v(x-\xi t)\right), \tag{67}$$

$$\Psi_7(x,t) = \frac{1}{\xi}\left(\delta-\Delta^2\beta^2-4\alpha\gamma\coth^2_\varepsilon\left(\frac{\sqrt{\beta^2-4\alpha\gamma}}{2}v(x-\xi t)\right)\right). \tag{68}$$

The mixed complex solitary wave solution is acquired,

$$\Phi_8(x,t) = \mp\imath\Delta\sqrt{\beta^2-4\alpha\gamma}\left(-\tanh_\varepsilon\left(\sqrt{\beta^2-4\alpha\gamma}\psi\right)\pm i\sqrt{mn}sech_\varepsilon\left(\sqrt{\beta^2-4\alpha\gamma}v(x-\xi t)\right)\right), \tag{69}$$

$$\Psi_8(x,t) = \frac{1}{\xi}\left(\delta-\Delta^2(\beta^2-4\alpha\gamma)\left(-\tanh_\varepsilon\left(\sqrt{\beta^2-4\alpha\gamma}\psi\right)\pm\sqrt{mn}sech_\varepsilon\left(\sqrt{\beta^2-4\alpha\gamma}v(x-\xi t)\right)\right)^2\right). \tag{70}$$

The mixed singular solutions are within the shape of,

$$\Phi_9(x,t) = \mp \imath\Delta\sqrt{\beta^2-4\alpha\gamma}\left(-\coth_\varepsilon\left(\sqrt{\beta^2-4\alpha\gamma}\psi\right) \pm i\sqrt{mn}csch_\varepsilon\left(\sqrt{\beta^2-4\alpha\gamma}v(x-\xi t)\right)\right), \tag{71}$$

$$\Psi_9(x,t) = \frac{1}{\xi}\left(\delta - \Delta^2\beta^2 - 4\alpha\gamma\left(-\coth_\varepsilon\left(\sqrt{\beta^2-4\alpha\gamma}\psi\right) \pm \sqrt{mn}csch_\varepsilon\left(\sqrt{\beta^2-4\alpha\gamma}v(x-\xi t)\right)\right)^2\right). \tag{72}$$

The mixed shock singular solutions are achieved along with shape of,

$$\Phi_{10}(x,t) = \pm\frac{\imath\Delta\sqrt{\beta^2-4\alpha\gamma}}{2}\left(\tanh_\varepsilon\left(\frac{\sqrt{\beta^2-4\alpha\gamma}}{4}\psi\right) + \coth_\varepsilon\left(\frac{\sqrt{\beta^2-4\alpha\gamma}}{4}v(x-\xi t)\right)\right), \tag{73}$$

$$\Psi_{10}(x,t) = \frac{1}{\xi}\left(\delta - \frac{\Delta^2\beta^2 - 4\alpha\gamma\left(\tanh_\varepsilon\left(\frac{\sqrt{\beta^2-4\alpha\gamma}}{4}\psi\right) + \sqrt{mn}\coth_\varepsilon\left(\frac{\sqrt{\beta^2-4\alpha\gamma}}{4}v(x-\xi t)\right)\right)^2}{4}\right). \tag{74}$$

(Class 3): As $\alpha\gamma > 0$ and $\beta = 0$, we obtained trigonometric solution as,

$$\Phi_{11}(x,t) = \pm\sqrt{\delta}\ tan_\varepsilon\left(\sqrt{\alpha\gamma}v(x-\xi t)\right), \tag{75}$$

$$\Psi_{11}(x,t) = \frac{\delta}{\xi}\left(1 + \tan^2_\varepsilon\left(\sqrt{\alpha\gamma}v(x-\xi t)\right)\right), \tag{76}$$

$$\Phi_{12}(x,t) = \mp\sqrt{\delta}\ cot_\varepsilon\left(\sqrt{\alpha\gamma}v(x-\xi t)\right), \tag{77}$$

$$\Psi_{12}(x,t) = \frac{\delta}{\xi}\left(1 + \cot^2_\varepsilon\left(\sqrt{\alpha\gamma}v(x-\xi t)\right)\right). \tag{78}$$

The mixed trigonometric solutions derived as,

$$\Phi_{13}(x,t) = \pm\sqrt{\delta}\left(\tan_\varepsilon\left(2\sqrt{\alpha\gamma}v(x-\xi t)\right) \pm \sqrt{mn}\ sec_\varepsilon\left(2\sqrt{\alpha\gamma}v(x-\xi t)\right)\right), \tag{79}$$

$$\Psi_{13}(x,t) = \frac{\delta}{\xi}\left(1 + \left(\tan_\varepsilon\left(2\sqrt{\alpha\gamma}v(x-\xi t)\right) \pm \sqrt{mn}\ sec_\varepsilon\left(2\sqrt{\alpha\gamma}v(x-\xi t)\right)\right)^2\right), \tag{80}$$

$$\Phi_{14}(x,t) = \pm\sqrt{\delta}\left(-\cot_\varepsilon\left(2\sqrt{\alpha\gamma}v(x-\xi t)\right) \pm \sqrt{mn}\ csc_\varepsilon\left(2\sqrt{\alpha\gamma}v(x-\xi t)\right)\right), \tag{81}$$

$$\Psi_{14}(x,t) = \frac{\delta}{\xi}\left(1 + \left(-\ cot_\varepsilon\left(2\sqrt{\alpha\gamma}v(x-\xi t)\right) \pm \sqrt{mn}\csc_\varepsilon\left(2\sqrt{\alpha\gamma}v(x-\xi t)\right)\right)^2\right), \tag{82}$$

$$\Phi_{15}(x,t) = \pm\frac{\sqrt{\delta}}{2}\left(\tan_\varepsilon\left(\frac{\sqrt{\alpha\gamma}}{2}v(x-\xi t)\right) - \cot_\varepsilon\left(\frac{\sqrt{\alpha\gamma}}{2}v(x-\xi t)\right)\right), \tag{83}$$

$$\Psi_{15}(x,t) = \frac{\delta}{\xi}\left(1 + \frac{1}{4}\left(\tan_\varepsilon\left(\frac{\sqrt{\alpha\gamma}}{2}v(x-\xi t)\right) - \cot_\varepsilon\left(\frac{\sqrt{\alpha\gamma}}{2}v(x-\xi t)\right)\right)^2\right). \tag{84}$$

(Class 4): As $\alpha\gamma < 0$ and $\beta = 0$, we obtained solutions with in the shape of shock solutions,

$$\Phi_{16}(x,t) = \mp\imath\sqrt{\delta}\left(\tanh_\varepsilon\left(\sqrt{-\alpha\gamma}v(x-\xi t)\right)\right), \tag{85}$$

$$\Psi_{16}(x,t)=\frac{\delta}{\xi}\left(1-tanh_{\varepsilon}^{2}\left(\sqrt{-\alpha\gamma}v(x-\xi t)\right)\right). \tag{86}$$

We obtain the singular solution as,

$$\Phi_{17}(x,t)=\mp\iota\sqrt{\delta}\left(\coth_{\varepsilon}\left(\sqrt{-\alpha\gamma}v(x-\xi t)\right)\right), \tag{87}$$

$$\Psi_{17}(x,t)=\frac{\delta}{\xi}\left(1-\coth_{\varepsilon}^{2}\left(\sqrt{-\alpha\gamma}v(x-\xi t)\right)\right). \tag{88}$$

The distinct solutions of complex combo type are derived as,

$$\Phi_{18}(x,t)=\pm\iota\sqrt{\delta}\left(-\tanh_{\varepsilon}\left(2\sqrt{-\alpha\gamma}v(x-\xi t)\right)\pm\sqrt{mn}sech_{\varepsilon}\left(2\sqrt{-\alpha\gamma}v(x-\xi t)\right)\right), \tag{89}$$

$$\Psi_{18}(x,t)=\frac{\delta}{\xi}\left(1-\left(-\tanh_{\varepsilon}\left(2\sqrt{-\alpha\gamma}v(x-\xi t)\right)\pm\sqrt{mn}sech_{\varepsilon}\left(2\sqrt{-\alpha\gamma}v(x-\xi t)\right)\right)^{2}\right), \tag{90}$$

$$\Phi_{19}(x,t)=\pm\iota\sqrt{\delta}\left(-\coth_{\varepsilon}\left(2\sqrt{-\alpha\gamma}v(x-\xi t)\right)\pm\sqrt{mn}csch_{\varepsilon}\left(2\sqrt{-\alpha\gamma}v(x-\xi t)\right)\right), \tag{91}$$

$$\Psi_{19}(x,t)=\frac{\delta}{\xi}\left(1-\left(-\coth_{\varepsilon}\left(2\sqrt{-\alpha\gamma}v(x-\xi t)\right)\pm\sqrt{mn}csch_{\varepsilon}\left(2\sqrt{-\alpha\gamma}v(x-\xi t)\right)\right)^{2}\right), \tag{92}$$

$$\Phi_{20}(x,t)=\pm\iota\frac{\sqrt{\delta}}{2}\left(\tanh_{\varepsilon}\left(\frac{\sqrt{-\alpha\gamma}}{2}v(x-\xi t)\right)+\coth_{\varepsilon}\left(\frac{\sqrt{-\alpha\gamma}}{2}v(x-\xi t)\right)\right), \tag{93}$$

$$\Psi_{20}(x,t)=\frac{\delta}{\xi}\left(1-\frac{1}{4}\left(\tanh_{\varepsilon}\left(\frac{\sqrt{-\alpha\gamma}}{2}v(x-\xi t)\right)+\coth_{\varepsilon}\left(\frac{\sqrt{-\alpha\gamma}}{2}v(x-\xi t)\right)\right)^{2}\right). \tag{94}$$

(Class 5): As $\alpha=\gamma$, and $\beta=0$, the periodic and mixed periodic solutions could be acquired in the configuration of periodic as well as mixed periodic class,

$$\Phi_{21}(x,t)=\pm\sqrt{\delta}\left(\tan_{\varepsilon}\left(\gamma v(x-\xi t)\right)\right), \tag{95}$$

$$\Psi_{21}(x,t)=\frac{\delta}{\xi}\left(1+\left(\tan_{\varepsilon}^{2}\left(\gamma v(x-\xi t)\right)\right)\right), \tag{96}$$

$$\Phi_{22}(x,t)=\pm\sqrt{\delta}\left(\cot_{\varepsilon}\left(\gamma v(x-\xi t)\right)\right), \tag{97}$$

$$\Psi_{22}(x,t)=\frac{\delta}{\xi}\left(1+\cot_{\varepsilon}^{2}\left(\gamma v(x-\xi t)\right)\right), \tag{98}$$

$$\Phi_{23}(x,t)=\pm\sqrt{\delta}\left(\tan_{\varepsilon}\left(2\gamma v(x-\xi t)\right)\pm\sqrt{mn}\sec_{\varepsilon}\left(2\gamma v(x-\xi t)\right)\right), \tag{99}$$

$$\Psi_{23}(x,t)=\frac{\delta}{\xi}\left(1+\left(\tan_{\varepsilon}\left(2\gamma v(x-\xi t)\right)\pm\sqrt{mn}\sec_{\varepsilon}\left(2\gamma v(x-\xi t)\right)\right)^{2}\right), \tag{100}$$

$$\Phi_{24}(x,t)=\pm\sqrt{\delta}\left(-\cot_{\varepsilon}\left(2\gamma v(x-\xi t)\right)\pm\sqrt{mn}\csc_{\varepsilon}\left(2\gamma v(x-\xi t)\right)\right), \tag{101}$$

$$\Psi_{24}(x,t)=\frac{\delta}{\xi}\left(1+\left(-cot_{\varepsilon}\left(2\gamma v(x-\xi t)\right)\pm\sqrt{mn}\csc_{\varepsilon}\left(2\gamma v(x-\xi t)\right)\right)^{2}\right), \tag{102}$$

$$\Phi_{25}(x,t) = \pm\frac{\sqrt{\delta}}{2}\left(\tan_\varepsilon\left(\frac{\gamma}{2}v(x-\xi t)\right) - \cot_\varepsilon\left(\frac{\gamma}{2}v(x-\xi t)\right)\right), \tag{103}$$

$$\Psi_{25}(x,t) = \frac{\delta}{\xi}\left(\frac{1}{4}\ \left(\tan_\varepsilon\left(\frac{\gamma}{2}v(x-\xi t)\right) - \cot_\varepsilon\left(\frac{\gamma}{2}v(x-\xi t)\right)\right)^2 + 1\right). \tag{104}$$

(Class 6): As $\beta = 0$ and $\gamma = -\alpha$, single as well as mixed wave composition have obtained with in following class,

$$\Phi_{26}(x,t) = \mp\imath\sqrt{\delta}\left(\tanh_\varepsilon\left(\alpha v(x-\xi t)\right)\right), \tag{105}$$

$$\Psi_{26}(x,t) = \frac{\delta}{\xi}\left(1 - \tanh^2_\varepsilon\left(\alpha v(x-\xi t)\right)\right), \tag{106}$$

$$\Phi_{27}(x,t) = \mp\imath\sqrt{\delta}\left(\coth_\varepsilon\left(\alpha v(x-\xi t)\right)\right), \tag{107}$$

$$\Psi_{27}(x,t) = \frac{\delta}{\xi}\left(1 - \coth^2_\varepsilon\left(\alpha v(x-\xi t)\right)\right), \tag{108}$$

$$\Phi_{28}(x,t) = \pm\imath\sqrt{\delta}\left(-\tanh_\varepsilon\left(\alpha v(x-\xi t)\right) \pm i\sqrt{mn}sech_\varepsilon\left(2\alpha v(x-\xi t)\right)\right)), \tag{109}$$

$$\Psi_{28}(x,t) = \frac{\delta}{\xi}\left(1 + \left(-\tanh_\varepsilon\left(2\alpha v(x-\xi t)\right) \pm i\sqrt{mn}sech_\varepsilon\left(2\alpha v(x-\xi t)\right)\right)^2\right), \tag{110}$$

$$\Phi_{29}(x,t) = \pm\imath\sqrt{\delta}\left(-\coth_\varepsilon\left(2\alpha v(x-\xi t)\right) \pm i\sqrt{mn}csch_\varepsilon\left(2\alpha v(x-\xi t)\right)\right)), \tag{111}$$

$$\Psi_{29}(x,t) = \frac{\delta}{\xi}\left(1 + \left(-\cot_\varepsilon\left(2\alpha v(x-\xi t)\right) \pm i\sqrt{mn}csch_\varepsilon\left(2\alpha v(x-\xi t)\right)\right)^2\right), \tag{112}$$

$$\Phi_{30}(x,t) = \mp\imath\frac{\sqrt{\delta}}{2}\left(\tanh_\varepsilon\left(\frac{\alpha}{2}v(x-\xi t)\right) + \coth_\varepsilon\left(\frac{\alpha}{2}v(x-\xi t)\right)\right), \tag{113}$$

$$\Psi_{30}(x,t) = \frac{\delta}{\xi}\left(1 - \frac{1}{4}\left(-\tanh_\varepsilon\left(\frac{\alpha}{2}v(x-\xi t)\right) + \coth_\varepsilon\left(\frac{\alpha}{2}v(x-\xi t)\right)\right)^2\right). \tag{114}$$

The (Class 7), (Class 8), (Class 9), (Class 10) have the constant solutions.
(Class 11): As $\alpha = 0$ and $\beta \neq 0$, the mixed hyperbolic solution have been created of the,

$$\Phi_{31}(x,t) = \mp\imath\sqrt{\delta}\left(1 - \frac{2m}{\left(\cosh_\varepsilon\left(\beta v(x-\xi t)\right) - \sinh_\varepsilon\left(\beta v(x-\xi t)\right) + m\right)}\right), \tag{115}$$

$$\Psi_{31}(x,t) = \frac{\delta}{\xi}\left(1 - \left(1 - \frac{2m}{\left(\cosh_\varepsilon\left(\beta v(x-\xi t)\right) - \sinh_\varepsilon\left(\beta v(x-\xi t)\right) + m\right)}\right)^2\right), \tag{116}$$

$$\Phi_{32}(x,t) = \mp\imath\sqrt{\delta}\left(1 - \frac{2\left(\sinh_\varepsilon\left(\beta v(x-\xi t)\right) + \cosh_\varepsilon\left(\beta v(x-\xi t)\right)\right)}{\left(\sinh_\varepsilon\left(\beta\psi\right) + \cosh_\varepsilon\left(\beta\psi\right) + n\right)}\right), \tag{117}$$

$$\Psi_{32}(x,t) = \frac{\delta}{\xi}\left(1 - \left(1 - \frac{2\left(\sinh_\varepsilon\left(\beta\psi\right) + \cosh_\varepsilon\left(\beta v(x-\xi t)\right)\right)}{\gamma\left(\sinh_\varepsilon\left(\beta\psi\right) + \cosh_\varepsilon\left(\beta v(x-\xi t)\right) + n\right)}\right)^2\right). \tag{118}$$

(Class 12): As $\gamma = pq,\ (q \neq 0),\ \beta = p$, and $\alpha = 0$, we gain plane solution as,

$$\Phi_{33}(x,t) = \mp\imath\sqrt{\delta}\left(1 - \frac{2qm\varepsilon^{pv(x-\xi t)}}{m - qn\varepsilon^{pv(x-\xi t)}}\right), \tag{119}$$

$$\Psi_{33}(x,t) = \frac{\delta}{\xi}\left(1 - \left(1 - \frac{2qm\varepsilon^{pv(x-\xi t)}}{m - qn\varepsilon^{pv(x-\xi t)}}\right)^2\right). \tag{120}$$

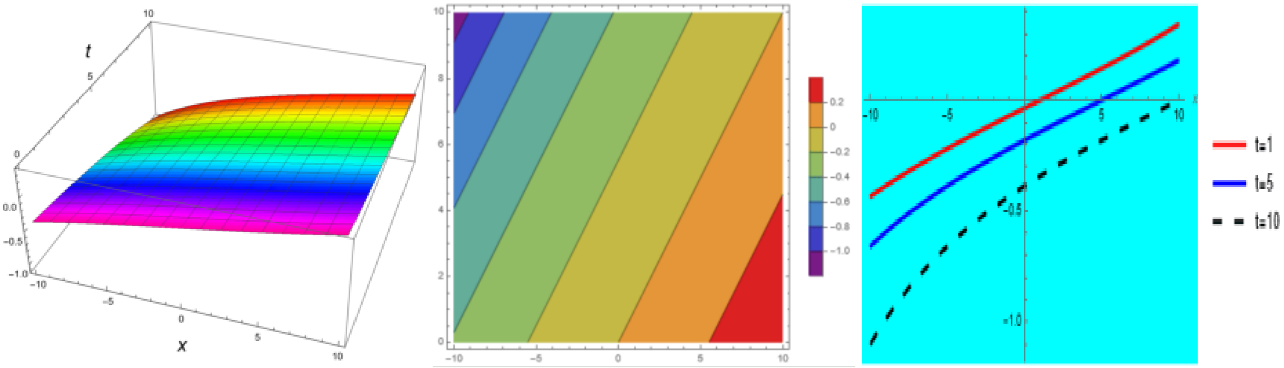

(a) 3D wave profile at wave number $v = 0.02$ **(b)** Contour wave profile at wave number $v = 0.02$ **(c)** 2D wave profile at wave number $v = 0.02$

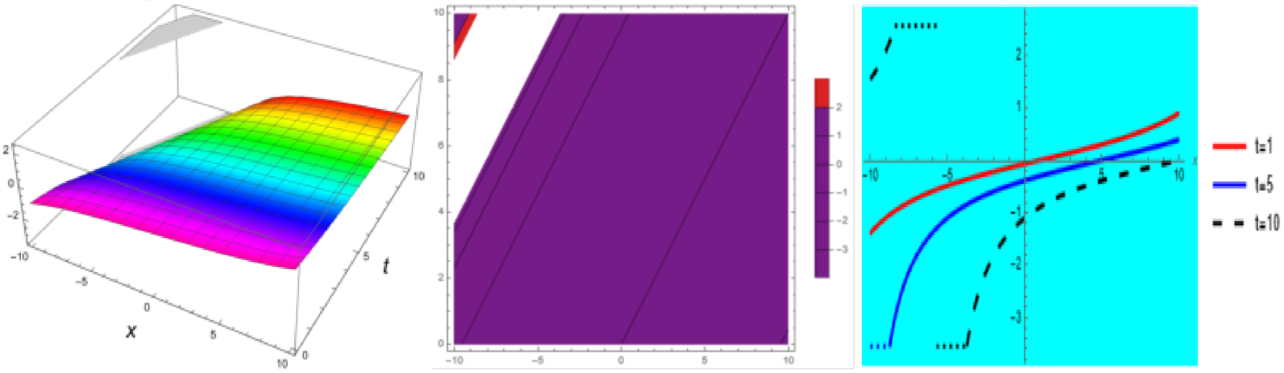

(d) 3D wave profile at wave number $v = 0.04$ **(e)** Contour wave profile at wave number $v = 0.04$ **(f)** 2D wave profile at wave number $v = 0.04$

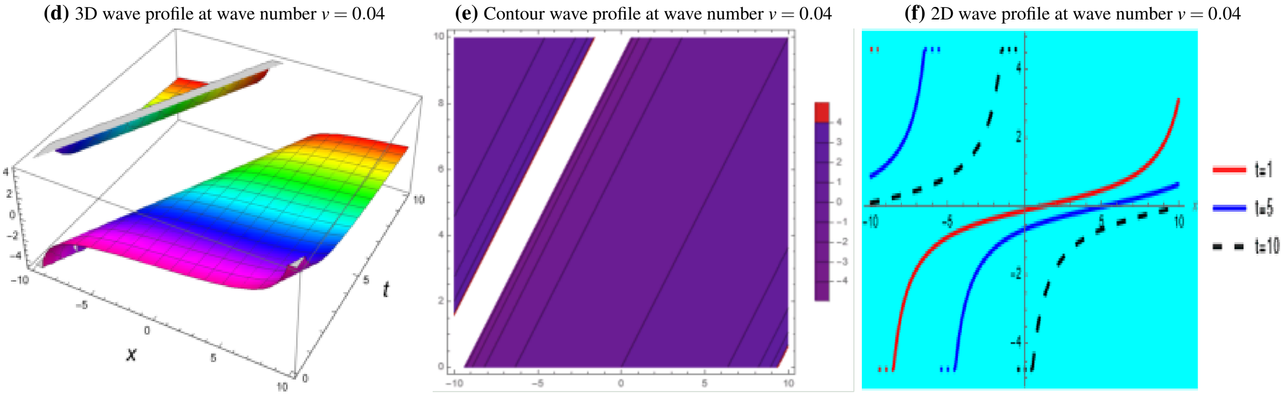

(g) 3D wave profile at wave number $v = 0.06$ **(h)** Contour wave profile at wave number $v = 0.06$ **(i)** 2D wave profile at wave number $v = 0.06$

Figure 1. Impact of wave number visualized through 3D, 2D and Contour for solution $\Phi_{21}(x,t)$

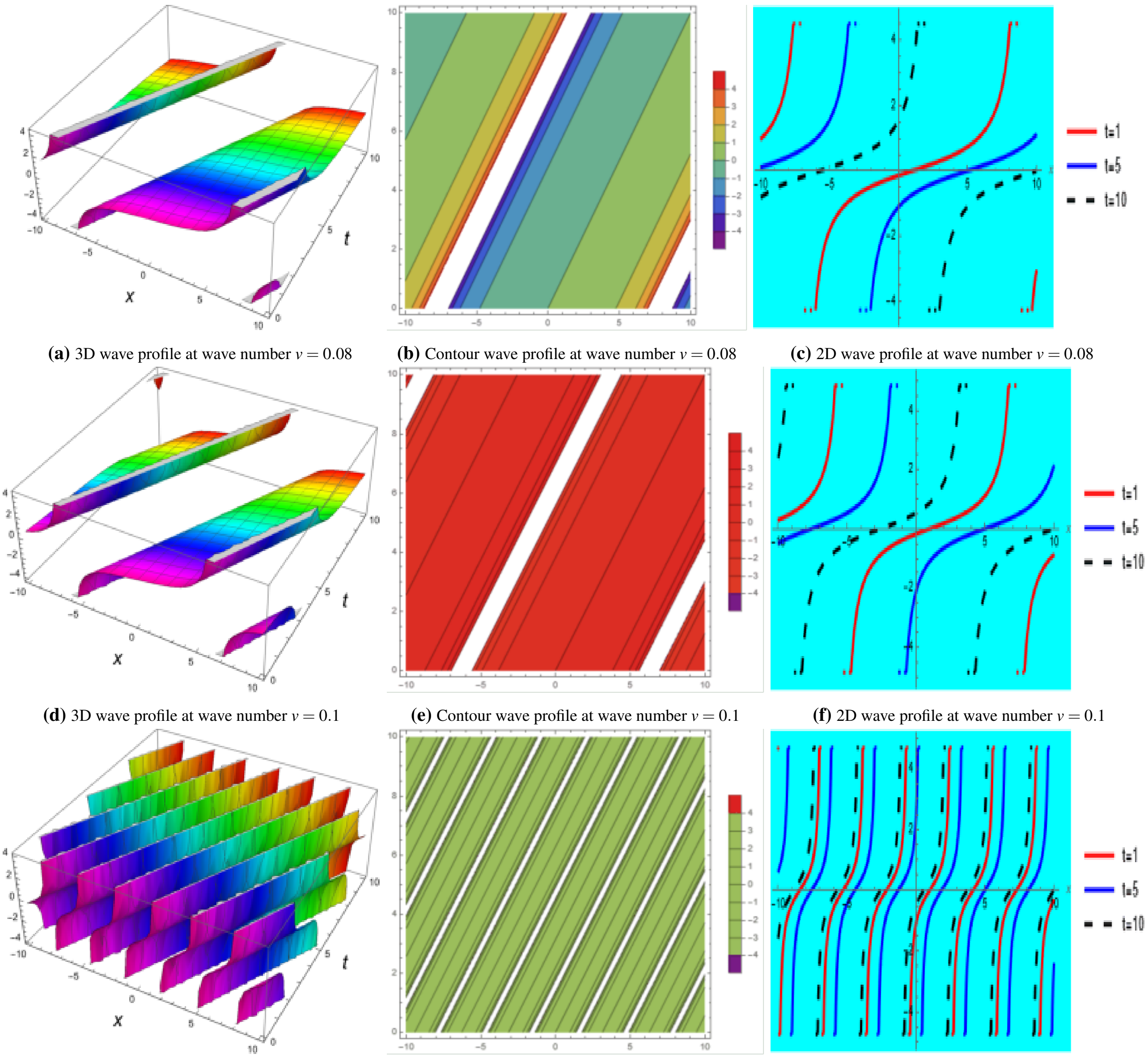

(a) 3D wave profile at wave number $v = 0.08$ **(b)** Contour wave profile at wave number $v = 0.08$ **(c)** 2D wave profile at wave number $v = 0.08$

(d) 3D wave profile at wave number $v = 0.1$ **(e)** Contour wave profile at wave number $v = 0.1$ **(f)** 2D wave profile at wave number $v = 0.1$

(g) 3D wave profile at wave number $v = 0.4$ **(h)** Contour wave profile at wave number $v = 0.4$ **(i)** 2D wave profile at wave number $v = 0.4$

Figure 2. Impact of wave number visualized through 3D, 2D and Contour for solution $\Phi_{21}(x,t)$

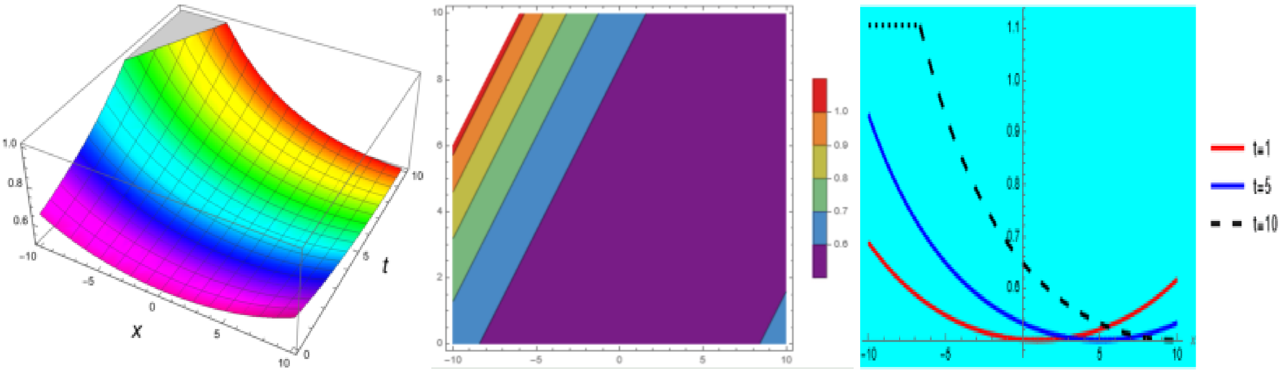

(a) 3D wave profile at wave number $v = 0.02$ **(b)** Contour wave profile at wave number $v = 0.02$ **(c)** 2D wave profile at wave number $v = 0.02$

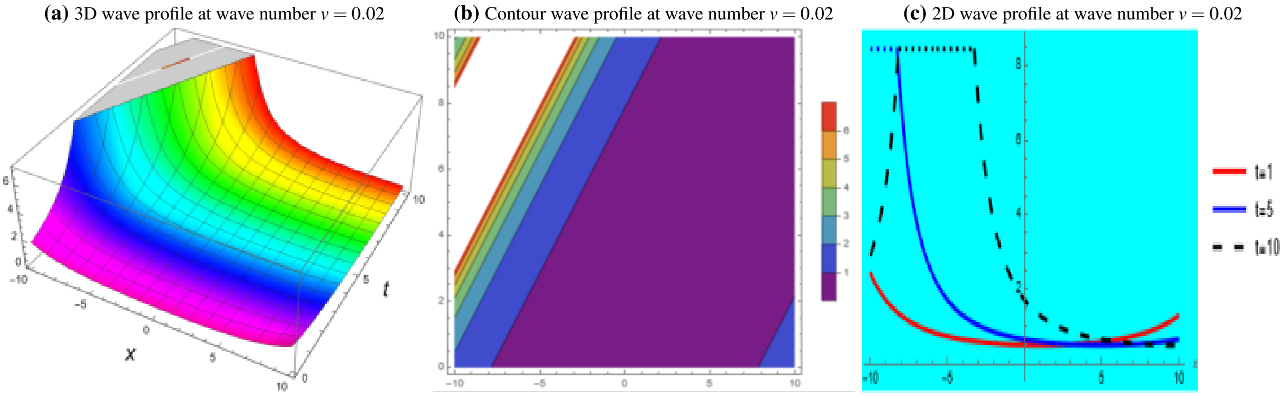

(d) 3D wave profile at wave number $v = 0.04$ **(e)** Contour wave profile at wave number $v = 0.04$ **(f)** 2D wave profile at wave number $v = 0.04$

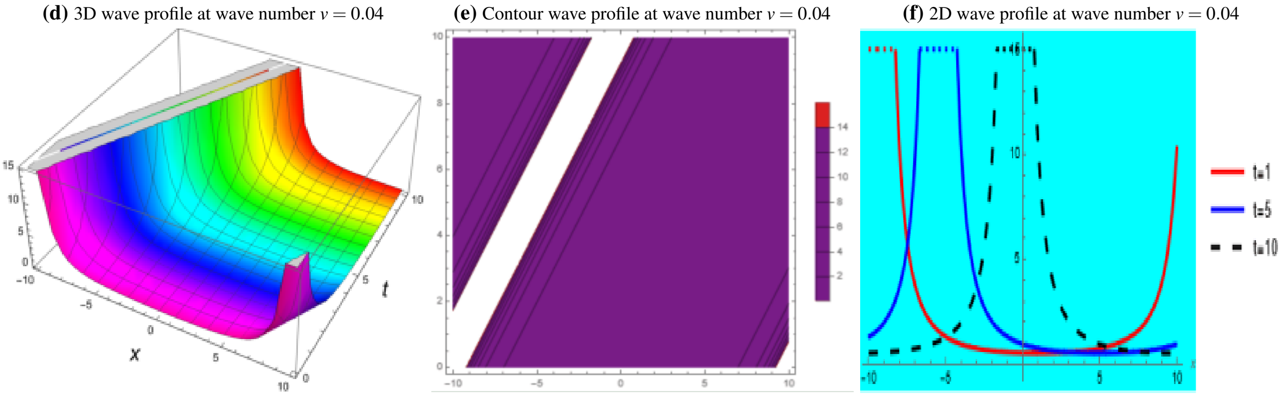

(g) 3D wave profile at wave number $v = 0.06$ **(h)** Contour wave profile at wave number $v = 0.06$ **(i)** 2D wave profile at wave number $v = 0.06$

Figure 3. Impact of wave number visualized through 3D, 2D and Contour for solution $\Psi_{21}(x,t)$

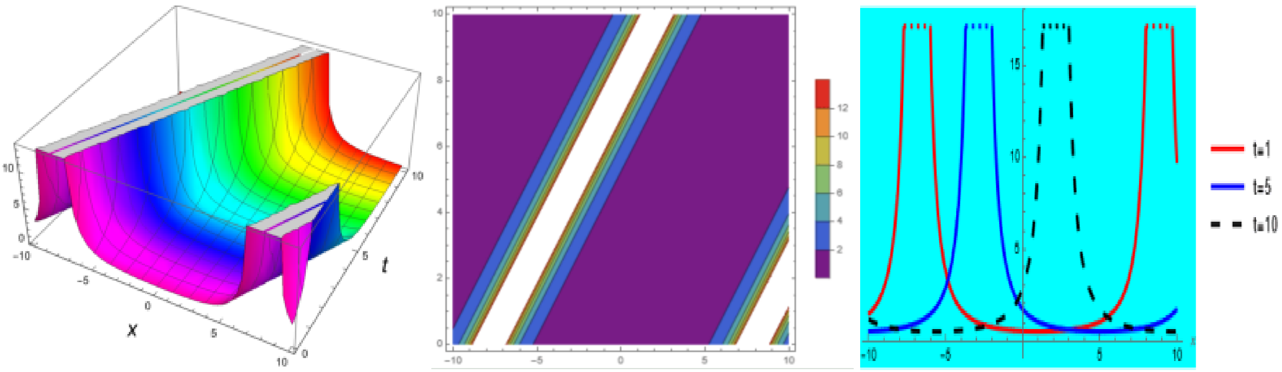

(a) 3D wave profile at wave number $v = 0.08$ **(b)** Contour wave profile at wave number $v = 0.08$ **(c)** 2D wave profile at wave number $v = 0.08$

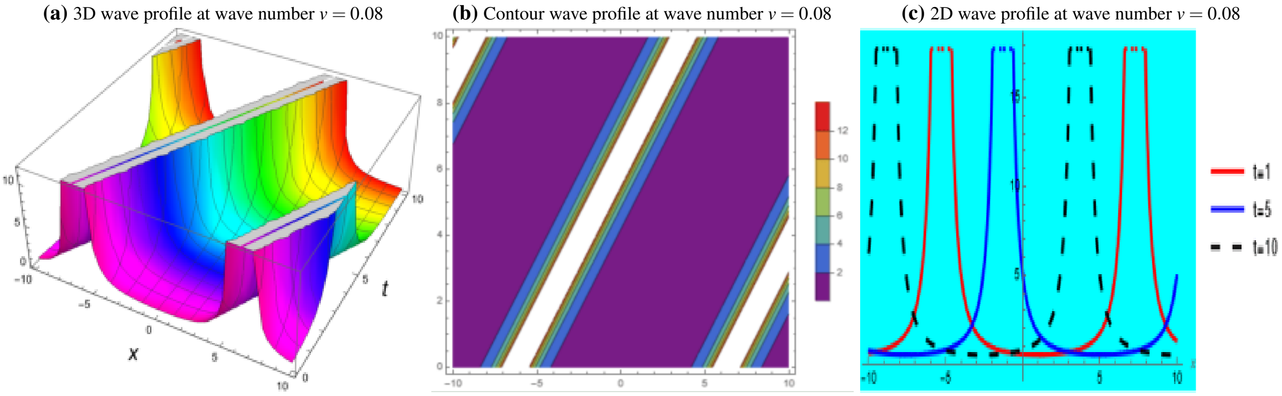

(d) 3D wave profile at wave number $v = 0.1$ **(e)** Contour wave profile at wave number $v = 0.1$ **(f)** 2D wave profile at wave number $v = 0.1$

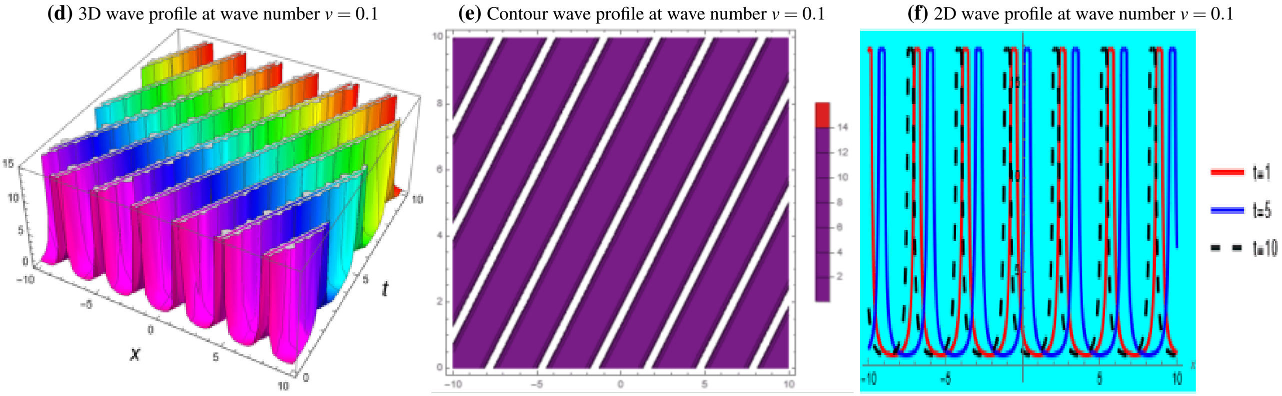

(g) 3D wave profile at wave number $v = 0.4$ **(h)** Contour wave profile at wave number $v = 0.4$ **(i)** 2D wave profile at wave number $v = 0.4$

Figure 4. Impact of wave number visualized through 3D, 2D and Contour for solution $\Psi_{21}(x,t)$

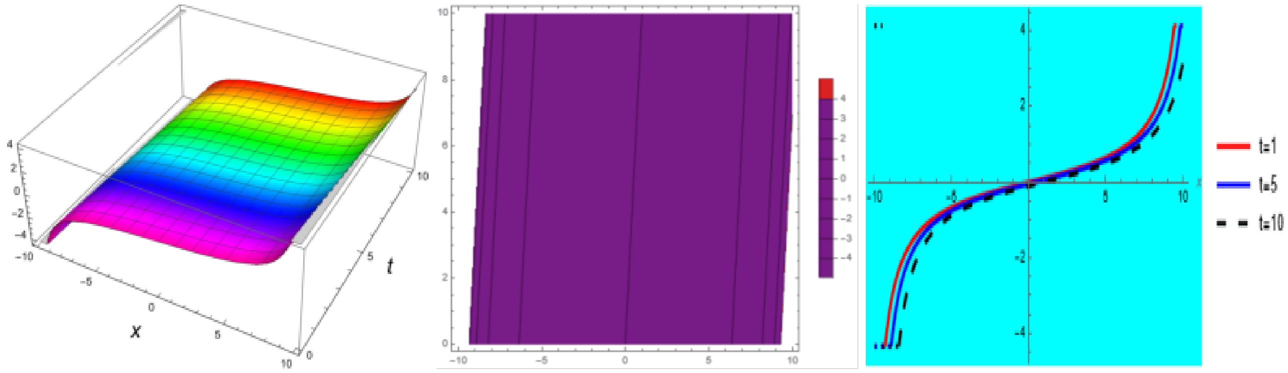

(a) 3D wave profile at velocity $\xi = 0.1$ **(b)** Contour visualization of wave number at velocity $\xi = 0.1$ **(c)** 2D wave profile at velocity $\xi = 0.1$

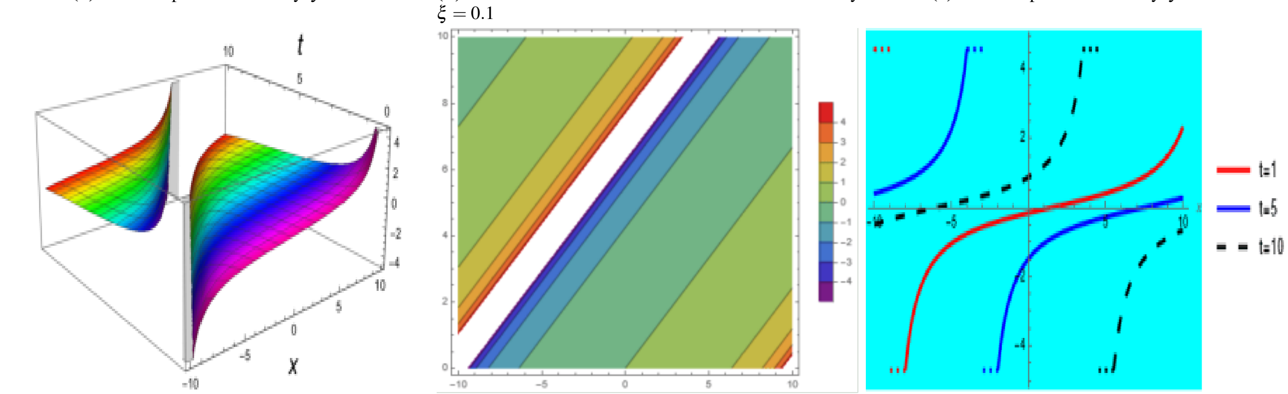

(d) 3D wave profile at velocity $\xi = 1.5$ **(e)** Contour wave profile at velocity $\xi = 1.5$ **(f)** 2D wave profile at velocity $\xi = 1.5$

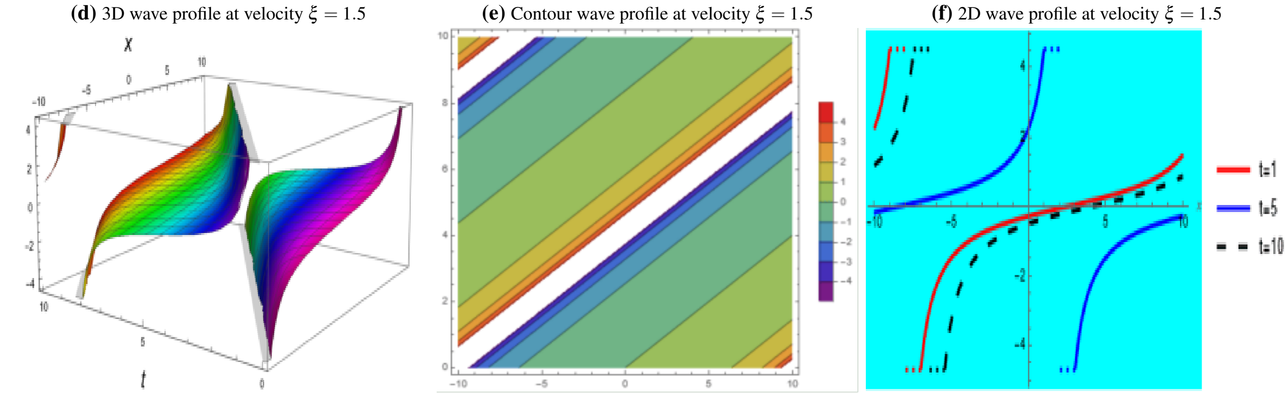

(g) 3D wave profile at velocity $\xi = 2.5$ **(h)** Contour wave profile at velocity $\xi = 2.5$ **(i)** 2D wave profile at velocity $\xi = 2.5$

Figure 5. Impact of velocity visualized through 3D, 2D and Contour for solution $\Phi_{21}(x,t)$

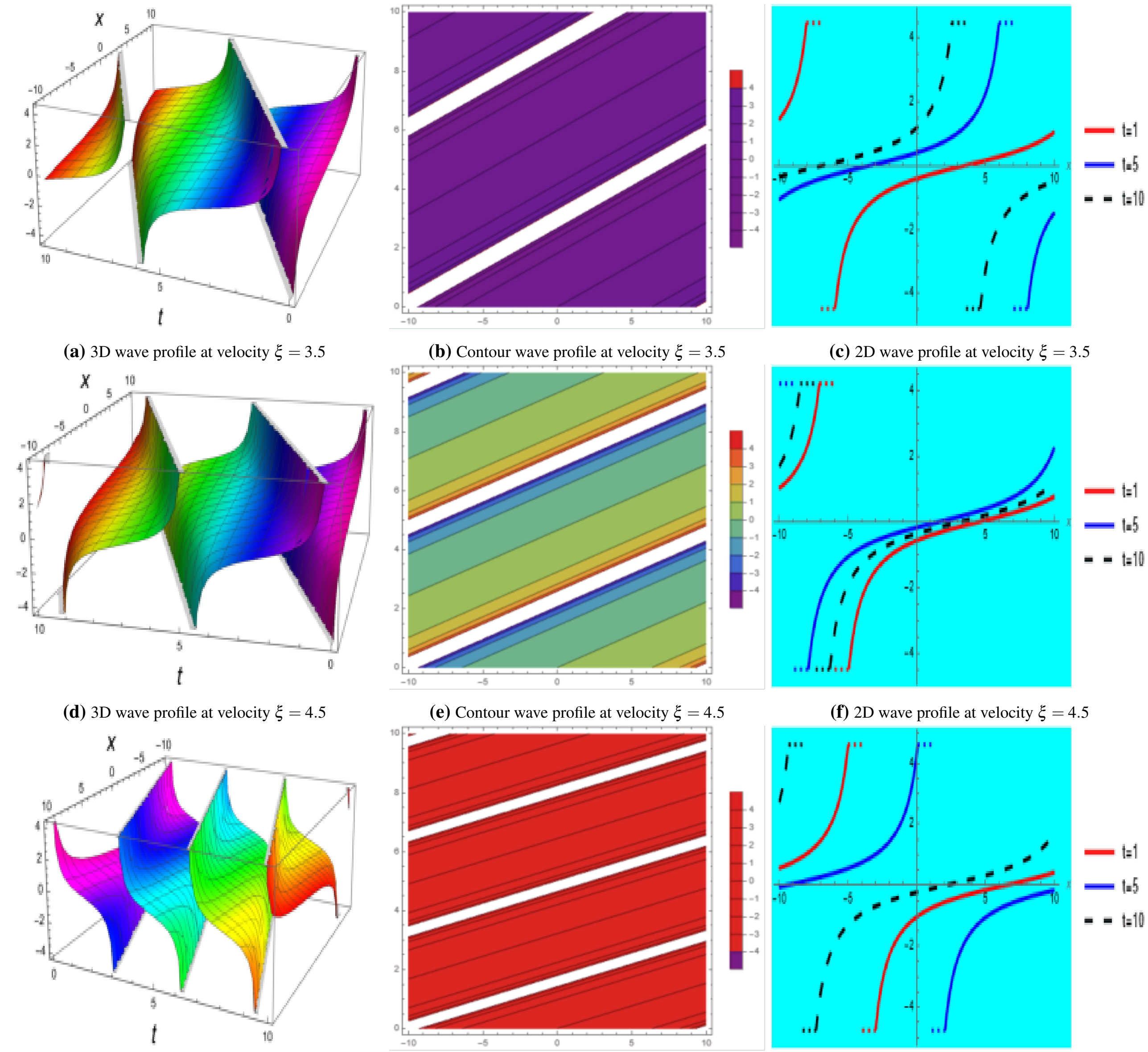

(a) 3D wave profile at velocity $\xi = 3.5$ **(b)** Contour wave profile at velocity $\xi = 3.5$ **(c)** 2D wave profile at velocity $\xi = 3.5$

(d) 3D wave profile at velocity $\xi = 4.5$ **(e)** Contour wave profile at velocity $\xi = 4.5$ **(f)** 2D wave profile at velocity $\xi = 4.5$

(g) 3D wave profile at velocity $\xi = 6.5$ **(h)** Contour wave profile at velocity $\xi = 6.5$ **(i)** 2D wave profile at velocity $\xi = 6.5$

Figure 6. Impact of velocity visualized through 3D, 2D and Contour for solution $\Phi_{21}(x,t)$

4.2 Application of Nucci's reduction method

In the present portion, we are applying Nucci's reduction method [60]. To utilize the technique, if we assume the variance of variables,
$K_1(\psi) = \mathbb{M}(\psi), K_2(\psi) = \mathbb{M}'(\psi)$,
then Eq. (49) can be transformed with is following of 1st order system ODEs:

$$\begin{aligned} \frac{dK_1}{d\psi} &= K_2, \\ \frac{dK_2}{d\psi} &= \frac{-2}{\xi^2 v^2}(K_1^3 + \delta K_1). \end{aligned} \tag{121}$$

Since, we could be choose K_1 as a another independent variable, now upper model is autonomous. Therefore, Eq. (121) reduces into,

$$\frac{dK_2}{dK_1} = \frac{-2}{\xi^2 v^2 K_2}(K_1^3 + \delta K_1). \tag{122}$$

The equation is separable ODE, along that ensuing exact result that can be one time integration concludes,

$$K_2(K_1) = \pm \frac{\sqrt{2\theta\xi^2 v^2 - K_1^4 - 2\delta K_1^2}}{\xi v}, \tag{123}$$

with θ is a arbitrary constant. The constant θ, evidently yields the ensuing 1st integral:

$$\theta = \frac{(\mathbb{M}'(\psi)\xi v)^2 + \mathbb{M}_1^4 + 2\delta\mathbb{M}_1^2}{2\xi^2 v^2}. \tag{124}$$

Substituting Eq. (123) into the first Eq. (121) yields,

$$\frac{dK_1(\xi)}{d\xi} = \pm \frac{\sqrt{2\theta\xi^2 v^2 - K_1^4 - 2\delta K_1^2}}{\xi v}, \tag{125}$$

it's a separable first order equation, too, as well as accordingly to general solution is, whenever $\theta \neq 0$:

$$\begin{aligned} \mathbb{M}(\psi) = K_1(\psi) = \pm \frac{\sqrt{2}}{\sqrt{\frac{\delta + \sqrt{2\theta\xi^2 v^2 + \delta^2}}{\theta\xi^2 v^2}}} \\ JacobiSN\left[\frac{\sqrt{\delta + \sqrt{2\theta\xi^2 v^2 + \theta^2\psi}}}{\xi v}, \sqrt{\frac{-\theta\xi^2 v^2 + \delta\sqrt{2\theta\xi^2 v^2 + \delta^2 - \delta^2}}{\theta\xi^2 v^2}}\right]. \end{aligned} \tag{126}$$

$$\begin{aligned} \Phi(x,t) = \pm \frac{\sqrt{2}}{\sqrt{\frac{\delta + \sqrt{2\theta\xi^2 v^2 + \delta^2}}{\theta\xi^2 v^2}}} \\ JacobiSN\left[\frac{\sqrt{\delta + \sqrt{2\theta\xi^2 v^2 + \theta^2\psi}}}{\xi v}, \sqrt{\frac{-\theta\xi^2 v^2 + \delta\sqrt{2\theta\xi^2 v^2 + \delta^2 - \delta^2}}{\theta\xi^2 v^2}}\right]. \end{aligned} \tag{127}$$

$$\begin{aligned} \Psi(x,t) = \frac{1}{\xi}\Bigg(\frac{2\theta\xi^2 v^2}{\delta + \sqrt{2\theta\xi^2 v^2 + \delta^2}} \\ \left[JacobiSN\,\frac{\sqrt{\delta + \sqrt{2\theta\xi^2 v^2 + \theta^2\psi}}}{\xi v}, \sqrt{\frac{-\theta\xi^2 v^2 + \delta\sqrt{2\theta\xi^2 v^2 + \delta^2 - \delta^2}}{\theta\xi^2 v^2}}\right]^2 + \delta\Bigg]. \end{aligned} \tag{128}$$

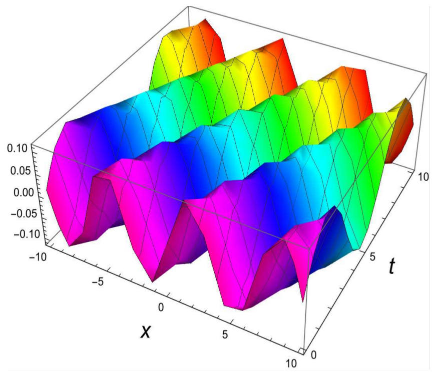

(a) A three-dimensional representation for wave number $v = 0.08$

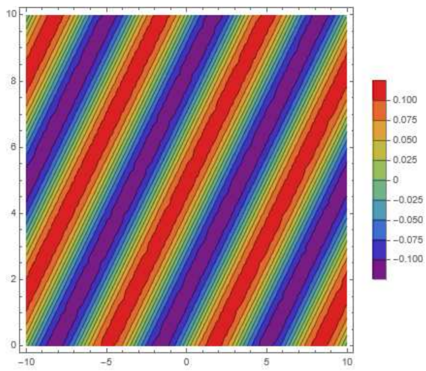

(b) Contour representation for wave number $v = 0.08$

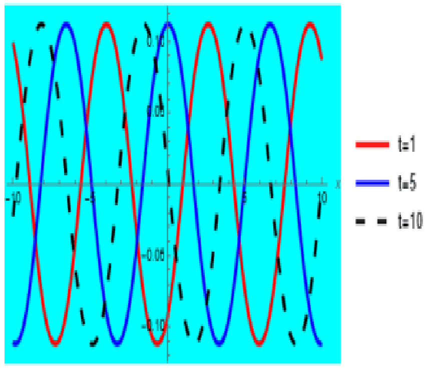

(c) A two-dimensional representation for wave number $v = 0.08$

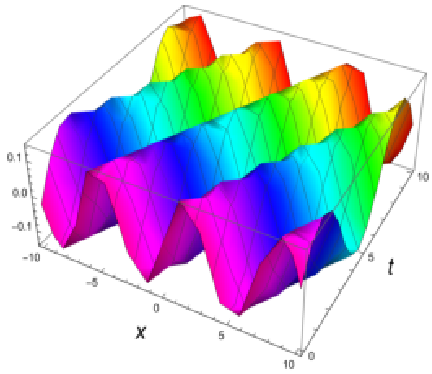

(d) A three-dimensional representation for wave number $v = 0.1$

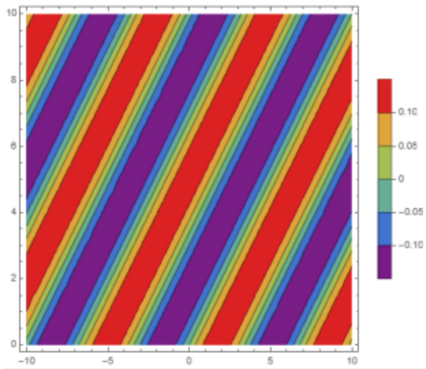

(e) Contour representation for wave number $v = 0.1$

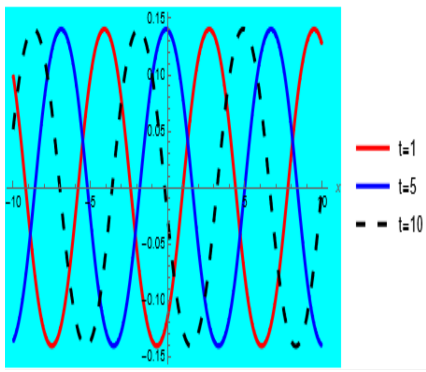

(f) A two-dimensional representation for wave number $v = 0.1$

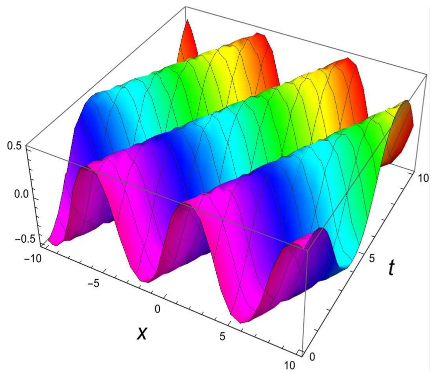

(g) A three-dimensional representation for wave number $v = 0.4$

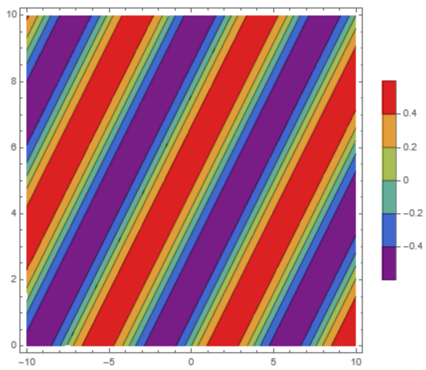

(h) Contour representation for wave number $v = 0.4$

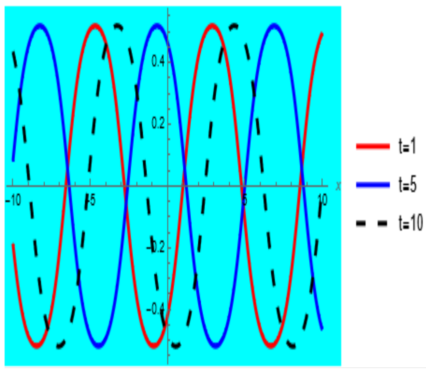

(i) A two-dimensional representation for wave number $v = 0.4$

Figure 7. Graphical representation of the wave number in 3D, 2D, and contour for the solution $\Phi_5(x,t)$

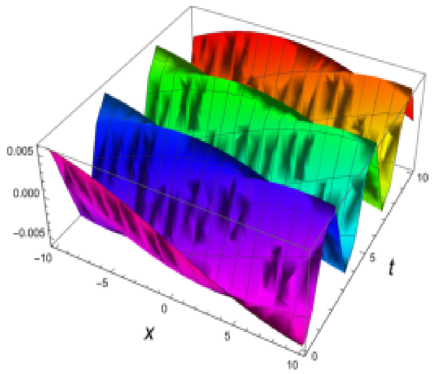

(a) A three-dimensional representation for velocity $\xi = 0.1$

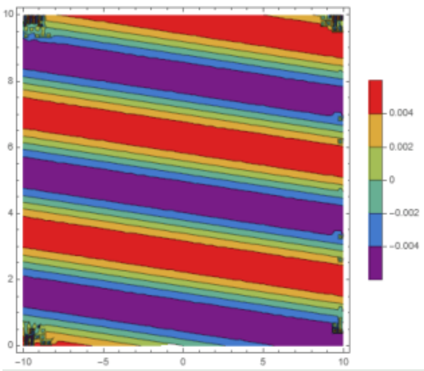

(b) Contour representation for velocity $\xi = 0.1$

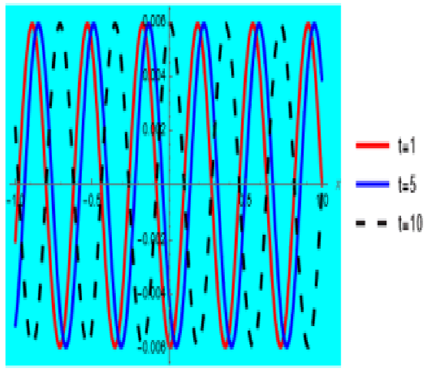

(c) A two-dimensional representation for velocity $\xi = 0.1$

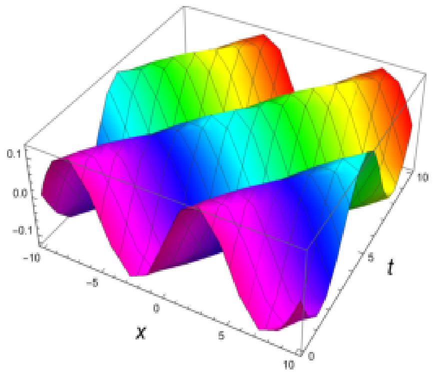

(d) A three-dimensional representation for velocity $\xi = 1.5$

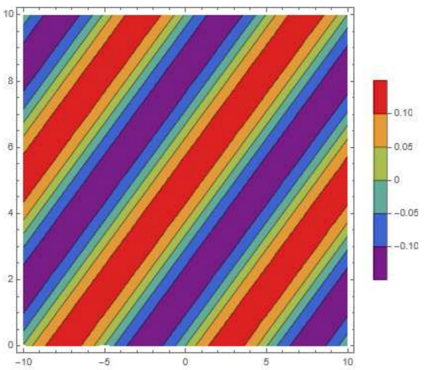

(e) Contour representation for velocity $\xi = 1.5$

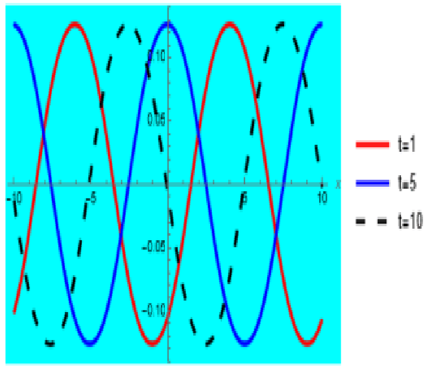

(f) A two-dimensional representation for velocity $\xi = 1.5$

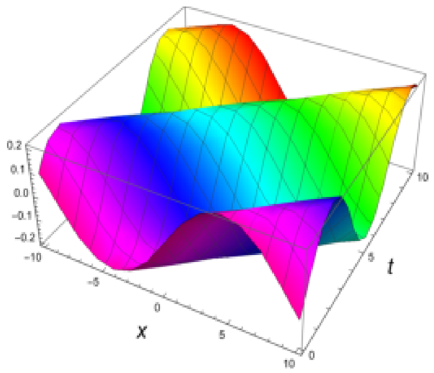

(g) A three-dimensional representation for velocity $\xi = 2.5$

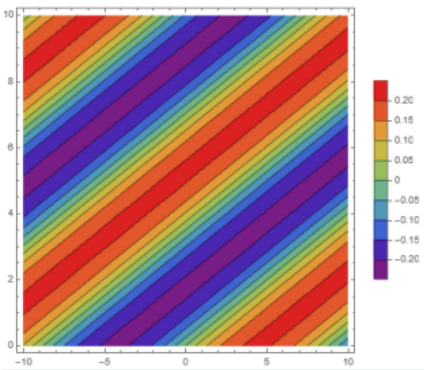

(h) Contour representation for velocity $\xi = 2.5$

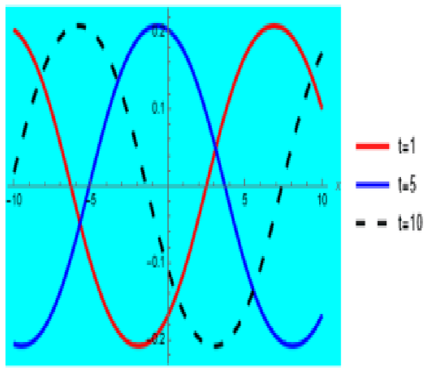

(i) A two-dimensional representation for velocity $\xi = 2.5$

Figure 8. Graphical representation of the velocity in 3D, 2D, and contour for the solution $\Phi_5(x,t)$

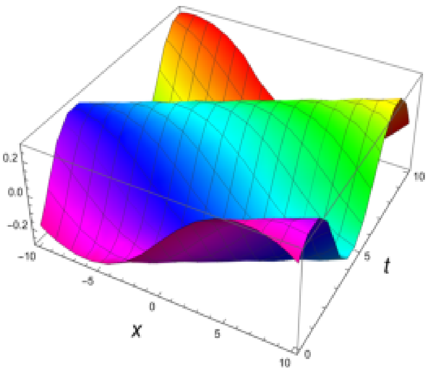

(a) A three-dimensional representation for velocity $\xi = 3.5$

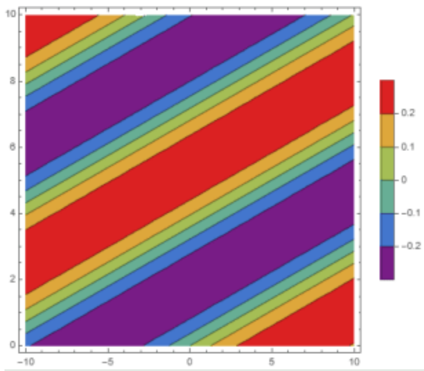

(b) Contour representation for velocity $\xi = 3.5$

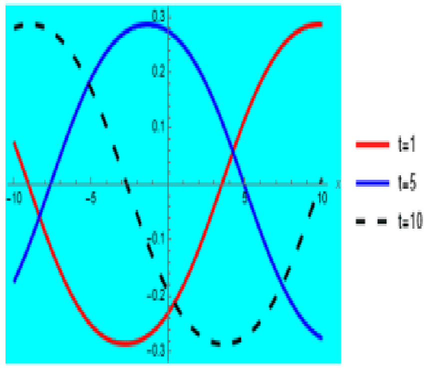

(c) A two-dimensional representation for velocity $\xi = 3.5$

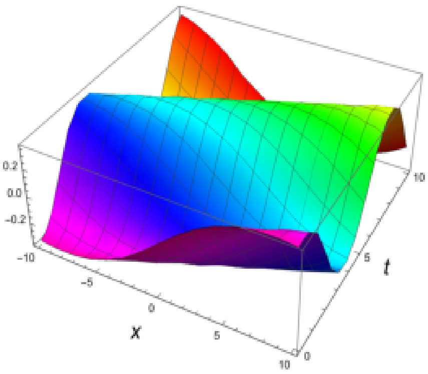

(d) A three-dimensional representation for velocity $\xi = 4.5$

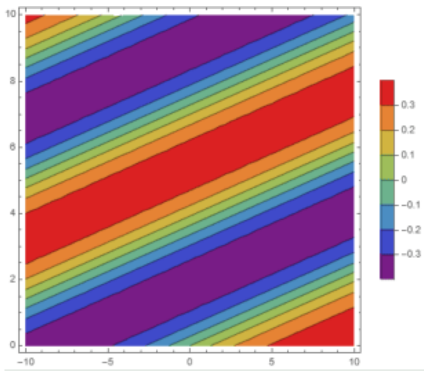

(e) Contour representation for velocity $\xi = 4.5$

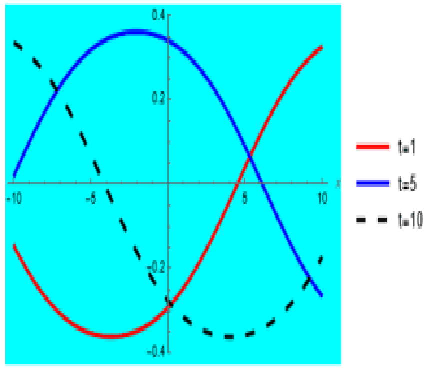

(f) A two-dimensional representation for velocity $\xi = 4.5$

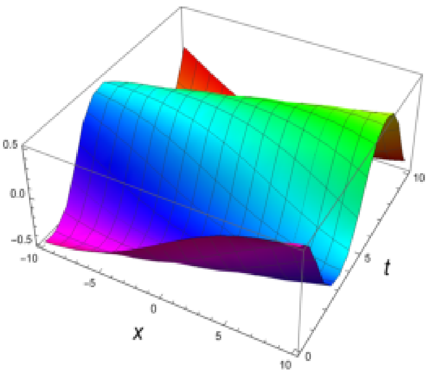

(g) A three-dimensional representation for velocity $\xi = 6.5$

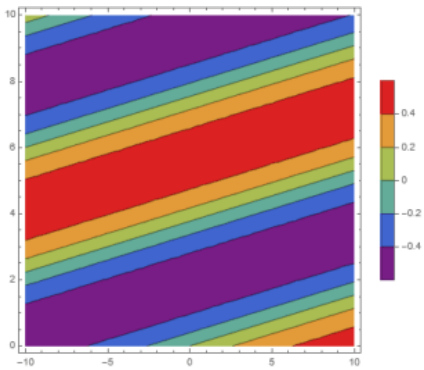

(h) Contour representation for velocity $\xi = 6.5$

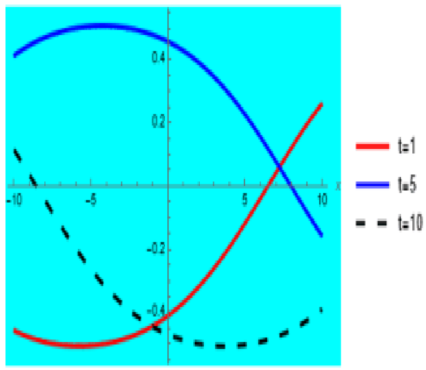

(i) A two-dimensional representation for velocity $\xi = 6.5$

Figure 9. Graphical representation of the wave number in 3D, 2D, and contour for the solution $\Phi_5(x,t)$

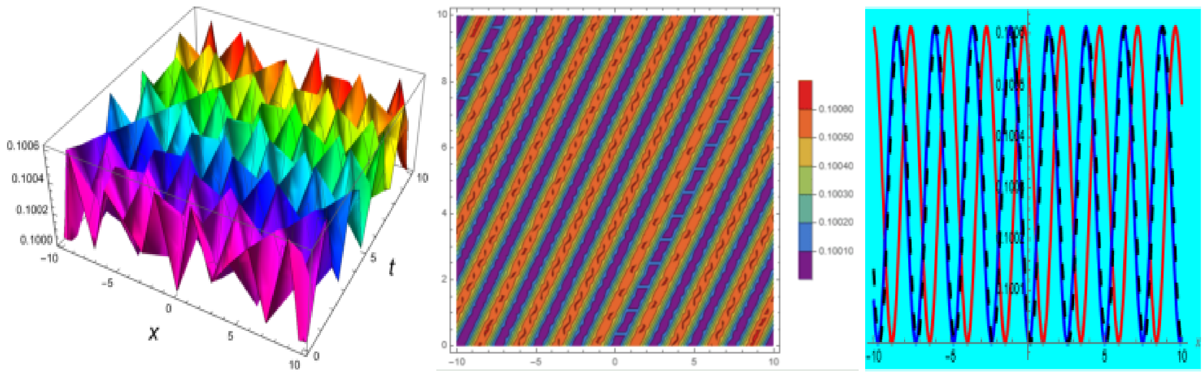

(a) A three-dimensional representation for wave number $v = 0.02$

(b) Contour representation at wave number $v = 0.02$

(c) A two-dimensional representation for wave number $v = 0.02$

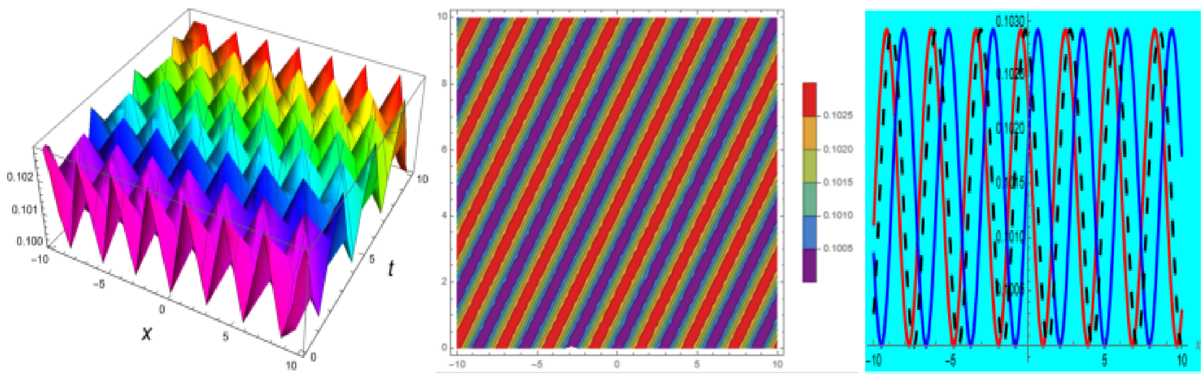

(d) A three-dimensional representation for wave number $v = 0.04$

(e) Contour representation at wave number $v = 0.04$

(f) A two-dimensional representation for wave number $v = 0.04$

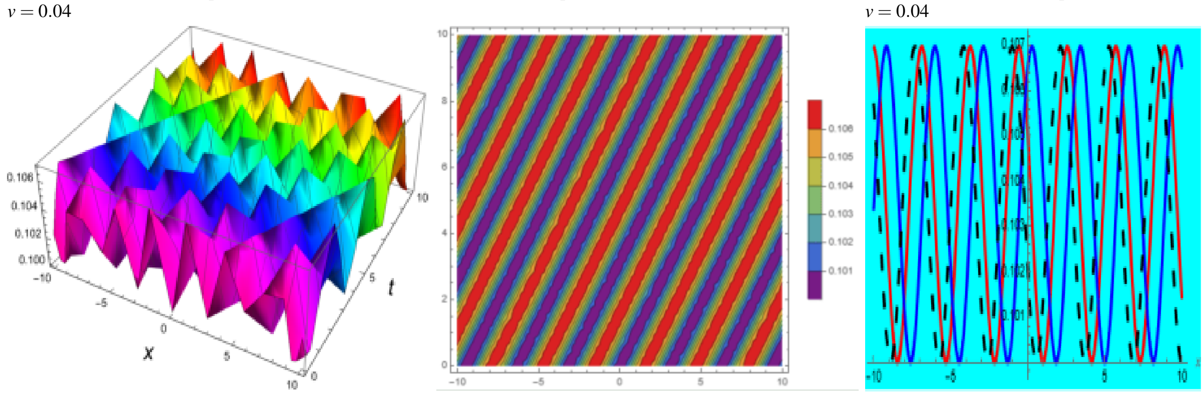

(g) A three-dimensional representation for wave number $v = 0.06$

(h) Contour representation at wave number $v = 0.06$

(i) A two-dimensional representation for wave number $v = 0.06$

Figure 10. Graphical representation of the wave number in 3D, 2D, and contour for the solution $\Psi_5(x,t)$

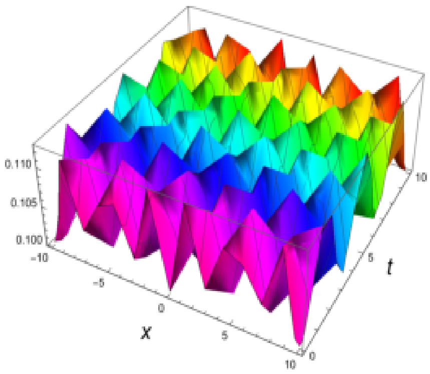

(a) A three-dimensional representation for wave number $v = 0.08$

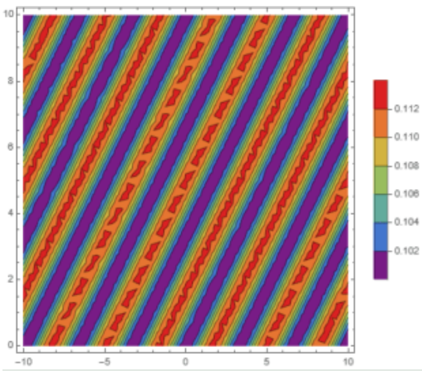

(b) Contour representation at wave number $v = 0.08$

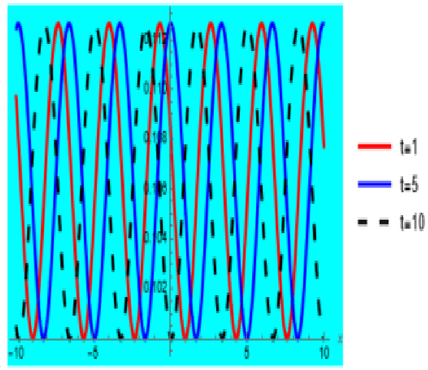

(c) A two-dimensional representation for wave number $v = 0.08$

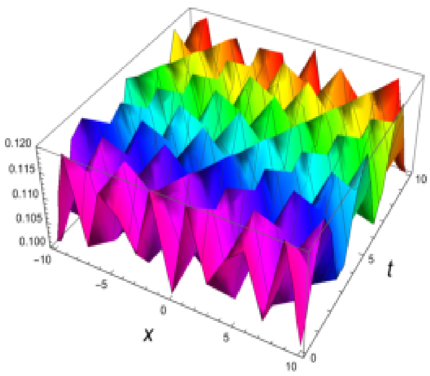

(d) A three-dimensional representation for wave number $v = 0.1$

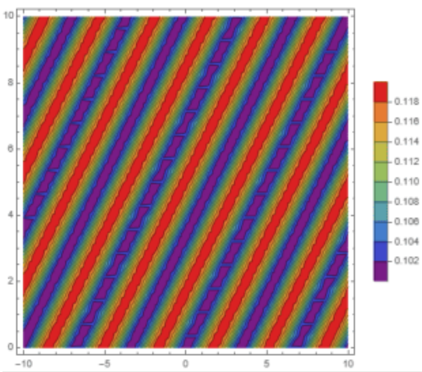

(e) Contour visualization at wave number $v = 0.1$

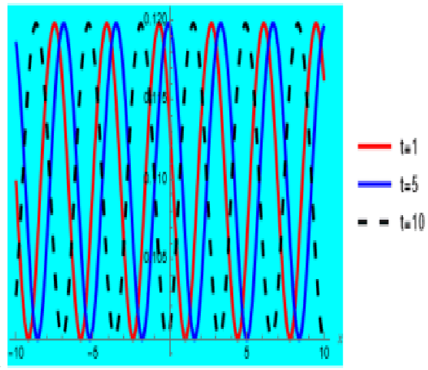

(f) A two-dimensional representation for wave number $v = 0.1$

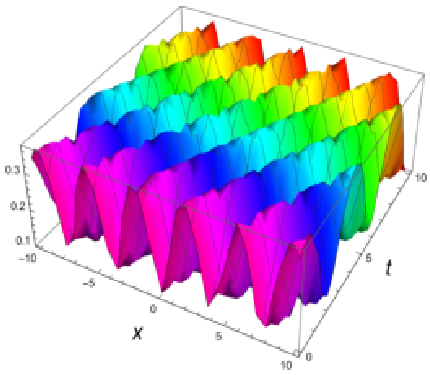

(g) A three-dimensional representation for wave number $v = 0.4$

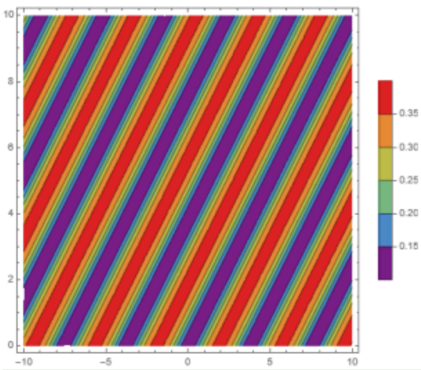

(h) Contour representation at wave number $v = 0.4$

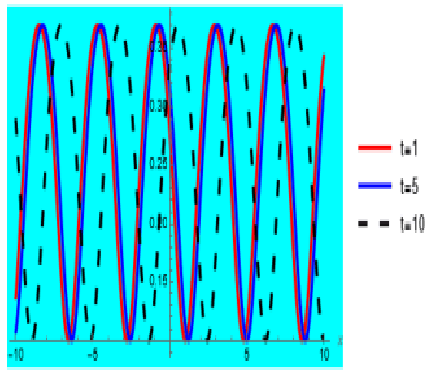

(i) A two-dimensional representation for wave number $v = 0.4$

Figure 11. Graphical representation of the wave number in 3D, 2D, and contour for the solution $\Psi_5(x,t)$

5. Graphical explanation

In this section, we discuss the results through various illustrative examples using different parameter values. This approach enables the identification of periodic waves, shock waves, singular waves, and complex solitary shocks. A magnetic shock wave, also known as a "magnetic compression wave," is a phenomenon observed in plasma and high-energy astrophysical environments. It involves rapid changes in the properties of the magnetic field, including its strength and direction. Magnetic shock waves are often accompanied by significant variations in plasma density, temperature, and pressure, and they play a crucial role in both astrophysical and laboratory plasma settings.

In the context of magnetic fields, complex solitary shocks typically occur in plasma environments, where the interactions between magnetic fields and plasma properties lead to intricate shock structures. These shocks involve not only rapid changes in plasma density, pressure, and velocity, but also in magnetic field strength and direction. The graphical representations presented in this section illustrate these phenomena, highlighting how waves can transmit energy across different points in space.

The picture of various specified out comes is concluded in 3-D, 2-D, and there associated contours by selecting various values for such parameter, $\gamma = 2.5$, $\delta = 0.5$, $\nu = 0.02$, $\xi = 1$. Fig. 1 and Fig. 2 are expressing the periodic along-with mixed periodic solution $\Phi_{21}(x,t)$ at wave number $\nu = 0.02, 0.04, 0.06, 0.08, 0.1, 0.4$ and wave velocity $\xi = 1$. Periodic and mixed periodic solutions in the context of magnetic fields are often associated with the behavior of charged particles (e.g., electrons or ions) in a magnetic field. When charged particles move in a uniform magnetic field, they can exhibit periodic motion. In more complex situations, charged particles can exhibit mixed behavior, including a combination of periodic and chaotic motion. The mixed periodic along with periodic outcomes could be acquired into the development of periodic and mixed periodic class. In Fig. 3 and Fig. 4 we tackle the same values for another solution and get the periodic and mixed periodic soliton. Fig. 5 and Fig. 6 we are increasing the value of velocity $\xi = 0.1, 1.5, 2.5, 3.5, 4.5, 6.5$ and wave number is $\nu = 0.06$ and acquired the results in the shape of periodic and mixed periodic soliton. These graphical representations provide a foundation for researchers to pursue diverse and advanced directions in their studies and applications. Fig. 7 and Fig. 8 we can show that the results into the shape of combined bright dark soliton and periodic soliton. In Fig. 9, Fig. 10 and Fig. 11, where the wave pattern of $\Phi(x,t)$ is bright-dark and the wave pattern of $\Psi(x,t)$ is periodic. This criteria is same for next figures, where the value of ξ, and ν is also same for the previous figures. The obtained results possess profound importance, benefiting not only physicians and chemists but also various industrial applications. These findings offer new avenues for research, enabling physicians to enhance their understanding of medical conditions and chemists to develop innovative solutions and compounds. While, also propelling progress at an industrial scale, with the promise of driving innovation and improvements in multiple sectors.

6. Modulation instability

6.1 Linear stability analysis

Into that portion, the purpose is to utilize linear stability analysis to establish the modulation instability (MI) of the governing system's (2) steady state solution. The MI might be consist of tiny optical wave phase or amplitude perturbations that develop rapidly over time. It is important to look into it with in nonlinear wave physics. In order to conduct the stability analysis, let's assume a steady state solution.

$$\Phi = \mathbf{X}_0, and\ \Psi = \mathbf{Y}_0, \tag{129}$$

where, $\mathbf{X}_0$ and $\mathbf{Y}_0$ are the initial incidence power (real constant amplitude). Further, outomes (129) is also transferring to perturbed stationary outcomes as,

$$\Phi = \mathbf{X}_0 + \varpi\Gamma(x,t), and\ \Psi = \mathbf{Y}_0 + \varpi\Pi(x,t), \tag{130}$$

where, Γ and Π are real functions of the x and t. The perturbation coefficient parameter is $\varpi << 1$. The disturbance equation is generated through inserting in the stationary perturbation outcomes into model 2.

$$\begin{aligned}
&\varpi \frac{\partial^2}{\partial x \partial t}\Gamma(x,t) - 2\mathbf{X}_0\mathbf{Y}_0 - 2\mathbf{X}_0\varpi\,\Pi(x,t) - 2\varpi\,\Gamma(x,t)\,\mathbf{Y}_0 - 2\varpi^2\Gamma(x,t)\,\Pi(x,t) = 0.\\
&\varpi \frac{\partial}{\partial t}\Gamma(x,t) + 2\varpi\left(\frac{\partial}{\partial x}\Gamma(x,t)\right)\mathbf{X}_0 + 2\varpi^2\left(\frac{\partial}{\partial x}\Gamma(x,t)\right)\Gamma(x,t) = 0.
\end{aligned} \tag{131}$$

After linearization, the disturbance Eq. (131) can be written as,

$$\begin{aligned}
&\varpi \frac{\partial^2}{\partial x \partial t}\Gamma(x,t) - 2\mathbf{X}_0\mathbf{Y}_0 - 2\mathbf{X}_0\varpi\,\Pi(x,t) - 2\varpi\,\Gamma(x,t)\,\mathbf{Y}_0 = 0.\\
&\varpi \frac{\partial}{\partial t}\Pi(x,t) + 2\varpi\left(\frac{\partial}{\partial x}\Gamma(x,t)\right)\mathbf{X}_0 = 0.
\end{aligned} \tag{132}$$

Forthwith, introduce a $\Gamma(x,t)$ and $\Pi(x,t)$, such as,

$$\begin{aligned}\Gamma(x,t) &= \mathbf{P}_1 e^{\imath(ax-bt)} + \mathbf{Q}_1 e^{-\imath(ax-bt)},\\ \Pi(x,t) &= \mathbf{P}_2 e^{\imath(ax-bt)} + \mathbf{Q}_2 e^{-\imath(ax-bt)}.\end{aligned} \tag{133}$$

The function (133) situate within (132) and obtain the model of homogeneous equations,

$$\begin{aligned}&ab\varpi\mathbf{P}_1 - 2\varpi\mathbf{P}_1\mathbf{Y}_0 - 2\varpi\mathbf{P}_2\mathbf{X}_0 = 0,\\ &ab\varpi\mathbf{Q}_1 - 2\varpi\mathbf{Q}_1\mathbf{Y}_0 - 2\varpi\mathbf{Q}_2\mathbf{X}_0 = 0,\\ &2\imath\mathbf{X}_0\varpi\mathbf{P}_1 a - \imath\varpi\mathbf{P}_2 b = 0,\\ &-2\imath\mathbf{X}_0\varpi\mathbf{Q}_1 a + \imath\varpi\mathbf{Q}_2 b = 0.\end{aligned} \tag{134}$$

The coefficient matrix of model (134) might be explicit like following $\mathbf{P}_1$, $\mathbf{P}_2$, $\mathbf{Q}_1$, also $\mathbf{Q}_2$,

$$\begin{pmatrix} ab\varpi - 2\varpi\mathbf{Y}_0 & 0 & -2\varpi\mathbf{X}_0 & 0\\ 0 & ab\varpi - 2\varpi\mathbf{Y}_0 & 0 & -2\varpi\mathbf{X}_0\\ 2\imath\mathbf{X}_0\varpi a & 0 & -\imath\varpi b & 0\\ 0 & -2\imath\mathbf{X}_0\varpi a & 0 & -\imath\varpi b\end{pmatrix}\begin{pmatrix}\mathbf{P}_1\\ \mathbf{Q}_1\\ \mathbf{P}_2\\ \mathbf{Q}_2\end{pmatrix} = \begin{pmatrix}0\\0\\0\\0\end{pmatrix}, \tag{135}$$

when the determinant disappears, the coefficient matrix (135) has nonlinear solutions. The dispersion relation obtain by expending the determinant of overhead coefficient matrix,

$$a^2b^4\varpi^4 - 8a^2b^2\varpi^4{X_0}^2 + 16a^2\varpi^4{X_0}^4 - 4ab^3\varpi^4Y_0 + 16ab\varpi^4{X_0}^2Y_0 + 4b^2\varpi^4{Y_0}^2, \tag{136}$$

$$b = \frac{\mathbf{Y}_0 + \sqrt{4a^2\mathbf{X}_2^2 + \mathbf{Y}_0^2}}{a},\ b = \frac{-\mathbf{Y}_0 + \sqrt{4a^2\mathbf{X}_2^2 + \mathbf{Y}_0^2}}{a}. \tag{137}$$

It can be observed that the coupled nonlinear system is modulational stable for any value of $\mathbf{X}_2$, $\mathbf{Y}_0$ and for all values of a except zero.

7. Conclusion

This study investigates the new coupled Konno-Oono (CKO) equation within the context of a magnetic field, focusing on the explicit solitonic structures derived using a novel extended algebraic equation mechanism and Nucci's reduction. These methods offer valuable insights and solutions applicable across a range of scientific and engineering disciplines. The study also examines modulational instability, a phenomenon in nonlinear media where wave amplitude grows over time, altering the wave's characteristics. This instability can evolve differently depending on the specific physical system and parameters involved. As a result,

- The proposed methods yield new, generalized, and distinct solutions to the current model, offering researchers a deeper understanding of complex phenomena, such as particle behavior in magnetic fields. This enhanced comprehension can lead to the development of more accurate models and improved predictive capabilities. The findings and methodologies established in this study have broad practical applications across various industries, ranging from healthcare to energy production.
- Applied analytical approaches are powerful tools for understanding and solving nonlinear phenomena. These methods offer exact, closed-form solutions, providing a precise understanding of the underlying dynamics. Analytical solutions are often more computationally efficient than numerical simulations, particularly for systems with well-behaved mathematical properties.
- The stability of the model is analyzed by calculating the modulational instability, which demonstrates that the model remains stable for all values of $\mathbf{X}_2$, $\mathbf{Y}_0$ and a. This indicates that, under the given conditions, the system does not exhibit any instability due to modulational effects, ensuring that the model's behavior is robust and consistent across these parameter ranges.
- These solutions are crucial for explaining specific physical phenomena in applied science. The new findings from this study are expected to be significant for key researchers and practitioners. The discovered solitary waves have important applications in various fields, including the modeling of oceanographic phenomena such as ocean gravity waves, as well as in other critical areas of research.

Acknowledgments
The authors extend their appreciation to Taif University, Saudi Arabia, for supporting this work through project number (TU-DSPP-2024-47).

Authors Contribution
Formal analysis: Umair Asghar. Funding acquisition: Yahya Alsayaad. Investigation: Umair Asghar. Methodology: Muhammad Imran Asjad Project administration: Yahya Alsayaad. Validation: Yasser Salah Hamed, Yahya Alsayaad. Visualization: Umair Asghar, Muhammad Imran Asjad Writing – review & editing: Muhammad Imran Asjad, Umair Asghar.

Availability of data and materials
Data sharing not applicable to this article as no data sets were generated or analyzed during the current study.

Conflict of interests
The authors declare that they have no known competing financial interests or personal relationships that could have appeared to influence the work reported in this paper.

References

[1] M. M. A. Khater, A. R. Seadawy, and D. Lu. "Dispersive solitary wave solutions of new coupled Konno-Oono, Higgs field and Maccari equations and their applications. ". *Journal of King Saud University-Science*, **30**:417–423, 2018.
DOI: https://doi.org/10.1016/j.jksus.2017.11.003.

[2] W. X. Ma and J. H. Lee. "A transformed rational function method and exact solutions to the 3+ 1 dimensional Jimbo–Miwa equation.". *Chaos, Solitons and Fractals*, **42**:1356–1363, 2009.
DOI: https://doi.org/10.1016/j.chaos.2009.03.043.

[3] W. X. Ma, T. Huang, and Y. Zhang. "A multiple exp-function method for nonlinear differential equations and its application.". *Physica scripta*, **82**: 065003, 2010.
DOI: https://doi.org/10.1088/0031-8949/82/06/065003.

[4] W. X. Ma and B. Fuchssteiner. "Explicit and exact solutions to a Kolmogorov-Petrovskii-Piskunov equation. ". *International Journal of Non-Linear Mechanics*, **31**:329–338, 1996.
DOI: https://doi.org/10.1016/0020-7462(95)00064-X.

[5] L. Cheng and W. X. Ma. "Similarity transformations and nonlocal reduced integrable nonlinear Schrödinger type equations.". *Mathematics*, **11**: 4110, 2023.

[6] M. A. E. Abdelrahman and H. A. Alkhidhr. "Fundamental solutions for the new coupled Konno-Oono equation in magnetic field.". *Results in Physics*, **19**:103445, 2020.
DOI: https://doi.org/10.1016/j.rinp.2020.103445.

[7] M. A. E. Abdelrahman and M. Kunik. "The ultra-relativistic Euler equations.". *Mathematical Methods in the Applied Sciences*, **38**:1247–1264, 2015.
DOI: https://doi.org/10.1002/mma.3141.

[8] M. A. E. Abdelrahman and M. Kunik. "On the shallow water equations.". *Zeitschrift für Naturforschung A*, **72**:873–879, 2017.
DOI: https://doi.org/10.1515/zna-2017-0146.

[9] M. A. E. Abdelrahman and M. A. Sohaly. "The development of the deterministic nonlinear PDEs in particle physics to stochastic case. ". *Results in Physics*, **9**:344–350, 2018.
DOI: https://doi.org/10.1016/j.rinp.2018.02.032.

[10] M. A. E. Abdelrahman and M. A. Sohaly. "Solitary waves for the nonlinear Schrödinger problem with the probability distribution function in the stochastic input case.". *The European Physical Journal Plus*, **132**:1–9, 2017.
DOI: https://doi.org/10.1140/epjp/i2017-11607-5.

[11] S. Z. Hassan and M. A. E. Abdelrahman. "A Riccati–Bernoulli sub-ODE method for some nonlinear evolution equations. ". *International Journal of Nonlinear Sciences and Numerical Simulation*, **20**:303–313, 2019.
DOI: https://doi.org/10.1515/ijnsns-2018-0045.

[12] P. Razborova, B. Ahmed, and A. Biswas. "Solitons, shock waves and conservation laws of Rosenau KdV RLW equation with power law nonlinearity.". *Applied Mathematics and Information Sciences*, **8**:485, 2014.
DOI: https://doi.org/10.12785/amis/080205.

[13] Sirendaoreji. "A new auxiliary equation and exact travelling wave solutions of nonlinear equations. ". *Physics Letters A*, **356**:124–130, 2006.
DOI: https://doi.org/10.1016/j.physleta.2006.03.034.

[14] X. Lü, L. L. Zhang, and W. X. Ma. "Oceanic shallow-water description with (2+ 1)-dimensional generalized variable-coefficient Hirota-Satsuma-Ito equation: Painlevé analysis, soliton solutions, and lump solutions.". *Physics of Fluids*, **36**, 2004.
DOI: https://doi.org/10.1063/5.0193477.

[15] L. L. Zhang, X. Lü, and S. Z. Zhu. "Painlevé analysis, Bäcklund transformation and soliton solutions of the (2+ 1)-dimensional variable-coefficient Boussinesq equation.". *International Journal of Theoretical Physics*, **63**:160, 2024.
DOI: https://doi.org/10.1007/s10773-024-05670-3.

[16] X. F. Yang, Z. C. Deng, and Y. Wei. "A Riccati-Bernoulli sub-ODE method for nonlinear partial differential equations and its application.". *Advances in Difference Equations*, **2015**:1–17, 2015.
DOI: https://doi.org/10.1186/s13662-015-0452-4.

[17] S. M. Ege and E. Misirli. "The modified Kudryashov method for solving some fractional-order non-linear equations.". *Advances in Difference Equations*, **2014**:1–13, 2014. URL http://www.advancesindifferenceequations.com/content/2014/1/135.

[18] S. Zhang. “A generalized exp-function method for fractional Riccati-differential equations. ”. *Drug Resistance Updates*, pages 48–51, 2010. URL https://sid.ir/paper/653406/en.

[19] W. X. Ma and Y. J. Zhang. “Darboux transformations of integrable couplings and applications.”. *Reviews in Mathematical Physics*, **30**:1850003, 2018.
DOI: https://doi.org/10.1142/S0129055X18500034.

[20] W.-X Ma. “Soliton solutions to sasa–satsuma-type modified Korteweg–de Vries equations by binary Darboux transformations.”. *Mathematics*, **12**: 3643, 2024.
DOI: https://doi.org/10.3390/math12233643.

[21] W.-X Ma. “A novel kind of reduced integrable matrix mKdV equations and their binary Darboux transformations.”. *Modern Physics Letters B*, **36**: 2250094, 2022.
DOI: https://doi.org/10.1142/S0217984922500944.

[22] W.-X Ma. “Binary Darboux transformation for general matrix mKdV equations and reduced counterparts.”. *Chaos, Solitons and Fractals*, **146**: 110824, 2021.
DOI: https://doi.org/10.1016/j.chaos.2021.110824.

[23] H. Bulut, T. A. Sulaiman, and H. M. Baskonus. “On the new soliton and optical wave structures to some non-linear evolution equations.”. *The European Physical Journal Plus*, **132**:1–11, 2017.
DOI: https://doi.org/10.1140/epjp/i2017-11738-7.

[24] H. Junqi. “An algebraic method exactly solving two high-dimensional nonlinear evolution equations.”. *Chaos, Solitons and Fractals*, **23**:391–398, 2005.
DOI: https://doi.org/10.1016/j.chaos.2004.02.044.

[25] S. S. Ray and S. Sahoo. “A novel analytical method with fractional complex transform for new exact solutions of time-fractional fifth-order Sawada-Kotera equation.”. *Reports on Mathematical Physics*, **75**:63–72, 2015.
DOI: https://doi.org/10.1016/S0034-4877(15)60024-6.

[26] F. S. Khodadad, F. Nazari, M. Eslami, and H. Rezazadeh. “Soliton solutions of the conformable fractional Zakharov–Kuznetsov equation with dual-power law nonlinearity. ”. *Optical and Quantum Electronics*, **49**:1–12, 2017.
DOI: https://doi.org/10.1007/s11082-017-1225-y.

[27] A. M. Wazwaz. “A sine-cosine method for handlingnonlinear wave equations.”. *Mathematical and Computer Modelling*, **40**:499–508, 2004.
DOI: https://doi.org/10.1016/j.mcm.2003.12.010.

[28] C. Dai and J. Zhang. “Jacobian elliptic function method for nonlinear differential-difference equations.”. *Chaos, Solitons and Fractals*, **27**: 1042–1047, 2006.
DOI: https://doi.org/10.1016/j.chaos.2005.04.071.

[29] M. A. E. Abdelrahman and H. A. Alkhidhr. “Fundamental solutions for the new coupled Konno-Oono equation in magnetic field. ”. *Results in Physics*, **19**:103445, 2020.
DOI: https://doi.org/10.1016/j.rinp.2020.103445.

[30] N. Faraz, Y. Khan, H. Jafari, A. Yildirim, and M. Madani. “Fractional variational iteration method via modified Riemann-Liouville derivative. ”. *Journal of King Saud University-Science*, **23**:413–417, 2011.
DOI: https://doi.org/10.1016/j.jksus.2010.07.025.

[31] B. Lu. “The first integral method for some time fractional differential equations. ”. *Journal of Mathematical Analysis and Applications*, **395**: 684–693, 2012.

[32] M. Eslami. “Trial solution technique to chiral non-linear Schrodinger’s equation in $(1+2)-$dimensions.”. *Nonlinear Dynamics*, **85**:813–816, 2016.
DOI: https://doi.org/10.1007/s11071-016-2724-2.

[33] A. Arnous, M. Ekici, S. Moshokoa, M. Zaka Ullah, A. Biswas, and M. Belic. “Solitons in nonlinear directional couplers with optical metamaterials by trial function scheme. ”. *Acta Physica Polonica A*, **132**:1399–1410, 2017.
DOI: https://doi.org/10.12693/APhysPolA.132.1399.

[34] A. Arnous, M. Ekici, S. Moshokoa, M. Zaka Ullah, A. Biswas, and M. Belic. “Variable coefficient-informed neural network for PDE inverse problem in fluid dynamics. ”. *Physica D: Nonlinear Phenomena*, page 134362, 2024.
DOI: https://doi.org/10.1016/j.physd.2024.134362.

[35] S. Chen and X. Lü. “Adaptive network traffic control with approximate dynamic programming based on a non-homogeneous Poisson demand model. ”. *Transportmetrica B: Transport Dynamics*, **12**:2336029, 2024.
DOI: https://doi.org/10.1080/21680566.2024.2336029.

[36] Y.-B. Su, X. Lü, S.-K. Li, L.-X. Yang, and Z. Gao. “Self-adaptive equation embedded neural networks for traffic flow state estimation with sparse data. ”. *Physics of Fluids*, **36**, 2024.
DOI: https://doi.org/10.1063/5.0230757.

[37] C. Han and X. Lü. “Novel patterns in the space variable fractional order Gray–Scott model. ”. *Nonlinear Dynamics*, **112**:16135–16151, 2024.
DOI: https://doi.org/10.1007/s11071-024-09857-5.

[38] F. Cao, X. Lü, Y.-X. Zhou, and X.-Y. Cheng. “Modified SEIAR infectious disease model for Omicron variants spread dynamics . ”. *Nonlinear Dynamics*, **111**:14597–14620, 2023.
DOI: https://doi.org/10.1007/s11071-023-08595-4.

[39] D. Gao, W.-X. Ma, and X. Lü. "Wronskian solution, Bäcklund transformation and Painlevé analysis to a (2+ 1)-dimensional Konopelchenko–Dubrovsky equation. ". *Zeitschrift für Naturforschung A*, **79**:887–895, 2024.
DOI: https://doi.org/10.1515/zna-2024-0016.

[40] K. Konno and H. Oono. "New coupled integrable dispersionless equations. ". *Journal of the Physical Society of Japan*, **63**:377–378, 1994.
DOI: https://doi.org/10.1143/jpsj.63.377.

[41] K. Konno and H. Kakuhata. "Novel solitonic evolutions in a coupled integrable, dispersionless system. ". *Journal of the Physical Society of Japan*, **65**:713–721, 1996.
DOI: https://doi.org/10.1143/JPSJ.65.713.

[42] A. Souleymanou, V. K. Kuetche, T. B. Bouetou, and T. C. Kofane. "Traveling wave-guide channels of a new coupled integrable dispersionless system. ". *Communications in Theoretical Physics*, **57**:10, 2012.
DOI: https://doi.org/10.1088/0253-6102/57/1/03.

[43] H. A. Alkhidhr and M. A. E. Abdelrahman. "Simulating new CKO as a model of seismic sea waves via unified solver. ". *Advances in Mathematical Physics*, **2023**, 2023.
DOI: https://doi.org/10.1155/2023/2514899.

[44] G. Yel, H. M.t Baskonus, and H. Bulut. "Novel archetypes of new coupled Konno-Oono equation by using sine-Gordon expansion method. ". *Optical and Quantum Electronics*, **49**:1–10, 2017.
DOI: https://doi.org/10.1007/s11082-017-1127-z.

[45] M. Shakeel, S. T. Mohyud-Din, and M. Asad Iqbal. "Modified extended exp-function method for a system of nonlinear partial differential equations defined by seismic sea waves ". *Pramana*, **91**:1–8, 2018.
DOI: https://doi.org/10.1007/s12043-018-1601-6.

[46] J. Manafian, I. Zamanpour, and A. Ranjbaran. "On some new analytical solutions for new coupled Konno-Oono equation by the external trial equation method. ". *Journal of Physics Communications*, **2**:015023, 2018.
DOI: https://doi.org/10.1088/2399-6528/aaa3a5.

[47] Md. A. Bashar, G. Mondal, K. Khan, and A. Bekir. "Traveling wave solutions of new coupled Konno-Oono equation. ". *New Trends in Mathematical Sciences*, **4**:296–303, 2016.
DOI: https://doi.org/10.20852/ntmsci.2016218536.

[48] H. Wang, K. Dong, F. Men, Y. J. Yan, and X. Wang. "Influences of longitudinal magnetic field on wave propagation in carbon nanotubes embedded in elastic matrix. ". *Zeitschrift für Naturforschung A*, **79**:887–895, 2024.
DOI: https://doi.org/10.1515/zna-2024-0016.

[49] I. Samir, N. Badra, H. M. Ahmed, and A. H. Arnous. "Solitons in birefringent fibers for CGL equation with Hamiltonian perturbations and Kerr law nonlinearity using modified extended direct algebraic method.". *Communications in Nonlinear Science and Numerical Simulation*, **102**:105945, 2021.
DOI: https://doi.org/10.1016/j.cnsns.2021.105945.

[50] A. H. Arnous, M. Mirzazadeh, L. Akinyemi, and A. Akbulut. "New solitary waves and exact solutions for the fifth-order nonlinear wave equation using two integration techniques.". *Journal of Ocean Engineering and Science*, **8**:475–480, 2022.
DOI: https://doi.org/10.1016/j.joes.2022.02.012.

[51] A. H. Arnous. "Optical solitons to the cubic quartic Bragg gratings with anti-cubic nonlinearity using new approach.". *Optik*, **251**:168356, 2022.
DOI: https://doi.org/10.1016/j.ijleo.2021.168356.

[52] R. Rodriguez, C. Santos, M. F. Simões, C. Soares, C. Santos, and N. Lima. "Polyphasic, including MALDI-TOF MS, evaluation of freeze-drying long-term preservation on Aspergillus (section Nigri) strains.". *Microorganisms*, **7**:291, 2019.
DOI: https://doi.org/10.3390/microorganisms7090291.

[53] X. Du. "Classification of single traveling wave solutions to the generalized strong nonlinear boussinesq equation without dissipation terms in P = 1.". *Journal of Applied Mathematics and Physics*, **2014**, 2014.
DOI: https://doi.org/10.4236/jamp.2014.23006.

[54] L. Cheng, Y. Zhang, and W.-X Ma. "An extended (2+ 1)-dimensional modified Korteweg–de Vries–Calogero–Bogoyavlenskii–Schiff equation: Lax pair and Darboux transformation.". *Communications in Theoretical Physics*, **77**:035002, 2024.
DOI: https://doi.org/10.1088/1572-9494/ad84d3.

[55] W. A. Faridi, U. Asghar, M. I. Asjad, A. M. Zidan, and S. M. Eldin. "Explicit propagating electrostatic potential waves formation and dynamical assessment of generalized Kadomtsev–Petviashvili modified equal width-Burgers model with sensitivity and modulation instability gain spectrum visualization.". *Results in Physics*, **44**:106167, 2023.
DOI: https://doi.org/10.1016/j.rinp.2022.106167.

[56] U. Asghar, W. A. Faridi, M. I. Asjad, and S. M. Eldin. "The enhancement of energy-carrying capacity in liquid with gas bubbles, in terms of solitons.". *Symmetry*, **14**:2294, 2014.
DOI: https://doi.org/10.3390/sym14112294.

[57] W.-X Ma. "A combined derivative nonlinear Schrödinger soliton hierarchy.". *Reports on Mathematical Physics*, **39**:313–325, 2024.
DOI: https://doi.org/10.1016/S0034-4877(24)00040-5.

[58] M. McAnally and W.-X Ma. "Explicit solutions and Darboux transformations of a generalized D-Kaup–Newell hierarchy.". *Nonlinear Dynamics*, **102**:2767–2782, 2020.
DOI: https://doi.org/10.1007/s11071-020-06030-6.

[59] H. Rezazadeh, M. Mirzazadeh, S. M. Mirhosseini-Alizamini, A. Neirameh, M. Eslami, and Q. Zhou. “Optical solitons of Lakshmanan–Porsezian–Daniel model with a couple of nonlinearities.”. *Optik*, **164**:414–423, 2018.
DOI: https://doi.org/10.1016/j.ijleo.2018.03.039.

[60] A. Akbulut, A. H. Arnous, M. S. Hashemi, and M. Mirzazadeh. “Solitary waves for the generalized nonlinear wave equation in (3+ 1) dimensions with gas bubbles using the Nnucci’s reduction, enhanced and modified Kudryashov algorithms.”. *Journal of Ocean Engineering and Science*, 2022.
DOI: https://doi.org/10.1016/j.joes.2022.07.002.